JAERI-Research
98-024

THE FATIGUE STRENGTH OF GRAPHITE AND CARBON MATERIALS FOR HTTR CORE COMPONENTS

March 1998

Motokuni ETO, Taketoshi ARAI and Takashi KONISHI*

日本原子力研究所
Japan Atomic Energy Research Institute

本レポートは，日本原子力研究所が不定期に公刊している研究報告書です。
入手の問合わせは，日本原子力研究所研究情報部研究情報課（〒319－1195 茨城県那珂郡東海村）あて，お申し越しください。なお，このほかに財団法人原子力弘済会資料センター（〒319－1195 茨城県那珂郡東海村日本原子力研究所内）で複写による実費頒布をおこなっております。

This report is issued irregularly.
Inquiries about availability of the reports should be addressed to Research Information Division, Department of Intellectual Resources, Japan Atomic Energy Research Institute, Tokai-mura, Naka-gun, Ibaraki-ken 〒319－1195, Japan.

編集兼発行　日本原子力研究所
印　　刷　日立高速印刷株式会社

JAERI-Research 98-024

The Fatigue Strength of Graphite and Carbon Materials for HTTR Core Components

Motokuni ETO, Taketoshi ARAI[+] and Takashi KONISHI [*]

Department of Materials Science and Engineering
Tokai Research Establishment
Japan Atomic Energy Research Institute
Tokai-mura,Naka-gun,Ibaraki-ken

(Received March 19,1998)

Room temperature fatigue tests were carried out on graphite and carbon meterials, which are used for the components in the core region of the HTTR, in the applied stress condition that R (= σ min／σ max) =− 3, − 1, 0 (PGX graphite) , =− 1, 0 (ASR-ORB carbon) and=− 1 (IG-11 graphite). The data were analyzed by Price's method, homologous stress method and P-T-S diagram method to investigate which is the most appropriate to derive desigh S-N curves. Fatigue tests were also carried out at 980 ℃ in vacuo on IG-11graphite to clarify the effect of temperature on its fatigue strength. The results indicated : (1) Price's method was the most appropriate to analyze the data for a design S-N curve. (2) Fatigue strength decreased with decreasing R-value,with the less pronounced tendency for ASR-ORB. (3) Design S-N curves were obtained on PGX and ASR-ORB on the basis of the data analyzed by Price's method. (4) Fatigue strength of IG-11 at 980 ℃ appeared to be almost the same as that for the room temperature fatigue strength, if the applied stress was normalized to the mean tensile strength at room temperature in vacuo.

Keywords : HTTR, Graphite,Carbon, Fatigue, Strength, Design Curve

---

+ Department of Advanced Nuclear Heat Technology, Oarai Research Establishment

* Toyo Tanso Co.,

HTTR炉心構造物用黒鉛及び炭素材料の疲労強度

日本原子力研究所東海研究所材料研究部
衛藤 基邦・荒井 長利[+]・小西 隆志[*]

(1998年3月19日受理)

HTTR炉心構造用黒鉛及び炭素材料について室温における疲労試験を実施した。応力負荷条件は応力比R((=σ min/σ max) =-3, -1, 0 (PGX黒鉛), =-1, 0 (ASR-ORB炭素) 及び=-1 (IG-11黒鉛) とした。取得したデータをPriceの方法、対応応力法及びP-T-S線図法によって解析し、設計疲労曲線を得るのに最適の方法を検討した。IG-11黒鉛については、980℃真空中で疲労試験を実施し、疲労強度に及ぼす温度の影響を調べた。主要な結論は次のとおりである。(1)設計疲労曲線を得るためにはPriceの方法が最も適している。(2)疲労強度はR値が小さいほど小さくなるが、この傾向はASR-ORBでは顕著ではない。(3)Priceの方法によってPGXとASR-ORBについて設計疲労曲線を得た。(4)980℃における IG-11の疲労強度は負荷応力を室温真空中の平均引張強度で規格化すると、室温における疲労強度とほぼ等しくなる。

東海研究所:〒319-1195 茨城県那珂郡東海村白方白根2-4

+ 大洗研究所核燃料利用研究部

* 東洋炭素株式会社

Contents

目　　次

1. Introduction

The components made of graphite and carbon materials in the HTTR, High Temperature Engineering Test Reactor, are subject to cyclic stresses caused by earthquakes, the variation in the pressure of coolant helium and thermal cycles during operation of the reactor [1-3]. Therefore, it is essential to obtain data on fatigue properties of the graphite and carbon materials for the design and sefety evaluation of the components. From the aspect of design of these components, it is a requisite to establish a fatigue strength diagram since the graphite structure design code for the HTTR requires the fatigue analysis [4].

There have been a number of investigations into the fatigue behavior of nuclear graphite. However, the fatigue data, in most cases, have shown large scatters so that it should be investigated what is the most appropriate statistical method to analyze the data.

Price [5] employed an assumption that logarithm of fatigue life be expressed by a linear equation of the logarithm of the ratio of the maximum applied tensile stress to the mean tensile strength, and that the deviation from the linear equation is to obey the normal distribution. His method gave rise to good agreement between the experiment and analysis for various loading modes. Wilkins et al. [6] , Ishiyama et al. [7,8] , and Eto et al. [9] used a concept of homologous stress to analyze the data points, and indicated that one can estimate the fatigue life even when the number of data points is small. There are another method to analyze the fatigue data, what is called P-T-S diagram method, in which a statistical distribution is assumed to be applied to the data on fatigue life at each stress level and the fatigue life as a function of stress level is plotted at a certain fatigue fracture probability [10].

The purpose of this report is to (1) summarize the fatigue data which have been obtained at room temperature on HTTR graphite and carbon materials, especially those used for the permanent reflector, plenum block and thermal insulator, for establishing the database, i, e., the data obtained in the test condition that the stress ratio R (= minimum applied stress σ_{min} / maximum applied stress σ_{max}) is 0.0, -1.0, and -3.0, and (2) to derive design fatigue curves from the results of analysis of the data by means of the methods mentioned above. In addition, the results of the fatigue test on a graphite for fuel block and sleeve at around 1000℃ were also summarized to make clear the effect of temperature on its fatigue strength, since the maximum temperature of coolant helium at the outlet is supposed to be 950℃ in the HTTR.

2. Experimental Procedure

2.1 Materials and specimens

Materials used were a fine-grained isotropic graphite IG-11 (Toyo Tanso Co.), semi-isotropic graphite PGX (UCAR) and a carbon material ASR-0RB (SIGRI), which are used as fuel sleeves, fuel blocks and replaceable reflectors; permanent reflectors and plenum blocks; and thermal insulating blocks at the core bottom; respectively. Some properties of these materials are summarized in Table 1. High temperature fatigue tests were done only for IG-11. The size of the original billets from which the smaller blocks were cut for the specimen preparation was 300×540×850 mm for IG-11 graphite, 1100 mm in diameter ×1220 mm in length for PGX graphite, and 1150 mm in diameter ×550 mm in length for ASR-0RB carbon. The size of the blocks from which specimens were machined was 155×155×500 mm for IG-11, 300×300×200 mm for PGX. A fan-shaped block with an angle of 45 degrees was used for specimens of ASR-0RB. Blocks in 115×115×400 mm were machined from the original billets of IG-11 for specimens to be used in the high temperature fatigue test.

Fig. 1 shows the size of an original block of IG-11 and the cutting plan for the specimen preparation. Table 1 summarizes mechanical properties of these materials. Dimensions of the specimen used in the present experiment are shown in Figs. 2 and 3 for room temperature and high temperature tests, respectively. For the room temperature test, specimens were machined either parallel to (L) or perpendicular to (T) the longitudinal axis of the blocks. Specimens for the test were selected randomly from all the specimens prepared except PGX graphite specimens for which the selection was carried out in the following way: First, the ultrasonic wave velocity was measured for all the specimens. Then, the Young's modulus, E, was estimated from the velocity, V and the mean value of apparent density (ρ = 1.74 g/cm^3), i. e., $E = \rho V^2$. The results of the estimation is :

	T-direction	L-direction
Number of specimens	228	228
Young's modulus (mean)	8.30 GPa	6.48 GPa
Standard deviation	0.54 GPa	0.42 GPa
Ultrasonic wave velocity (mean)	2182 m/s	1928 m/s

Specimens which displayed the ultrasonic wave velocity smaller than the mean value by 200 m/s or more, i. e., 0.70 GPa for the Young's modulus, were deleted from the specimens for the test. The number of specimens deleted was 19 (8.3%) and 23 (10.1%) for T- and L-directions, respectively.

Specimens for the high temperature test were cut from 6 blocks shown in Fig. 1 in the way that their longitudinal axis was parallel to the longitudinal axis of the blocks. No selection was made on specimens for the high temperature test.

2.2 Tensile and compressive tests

Since there had been no data available on the effect of specimen size on the tensile and compressive strengths of PGX graphite, tensile and compressive tests were carried out on specimens with several sizes. For the tensile test three kinds of dumbbell type specimens were used: 5 mm in diameter ×20 mm in gage length, 10 mm in diameter ×20 mm in gage length, and 20 mm in diameter ×20 mm in gage length. For the compressive test, five kinds of cylindrical specimens were used: 5 mm in diameter ×10 mm in length, 10 mm in dia. ×20 mm in length, 15 mm in dia. ×30 mm in length, 30 mm in dia. ×60 mm in length, and 50 mm in dia. ×100 mm in length . A screw-driven test machine was used for these tests at a cross-head speed of 0.1 mm/min. For the compressive test, 2 mm thick sheets of teflon were placed between a specimen and the upper and lower compression plates to reduce the friction.

2.3 Fatigue tests

To determine the applied stress for the fatigue test tensile tests were carried out for fatigue specimens of all the three materials, using a servohydraulic test machine. The number of specimens tested ranged from 20 to 40. Before the high temperature fatigue test tensile tests were also done on specimens shown in Fig. 3 at room temperature and 980℃ in vacuo using a servohydraulic test machine with the maximum allowable load of about 100 kN. The number of specimens tested was 5 for both room temperature and 980℃.

Room temperature fatigue tests were carried out in the loading condition that R (= σ_{min}/ σ_{max}) values were 0, -1, and -3 (L-direction of PGX graphite only). Several levels of the tensile applied stress were chosen, ranging from 0.7 to 1.0 of the mean static tensile strength. The loading speed was 8.75×10^3 N/s, 2.62×10^3 N/s, and 2.13×10^3 N/s for IG-11, PGX and ASR-0RB, respectively. The clyclic load in the triangular wave was applied to the specimen up to failure or 10^5 cycles.

High temperature fatigue tests were carried out in the loading condition that the maximum applied stress level was 0.75 to 0.9 of the mean tensile strength with R~ 0.0. The frequency of the cyclic stress was about 1 Hz. In some cases the fatigue test was carried out to more than 10^5 cycles. Those specimens which survived after 10^5 or more cycles of repeated stresses were subject to tensile tests at room temperature.

3. Results and Discussion

3.1 Volume dependence of tensile and compressive strengths

Data on the effect of specimen volume on the tensile and compressive strengths of IG-11 graphite were already summarized in the previous study, indicating that the size of the fatigue specimen employed here is appropriate [9].

The data on strength of PGX graphite measured in the present study are shown in Fig. 4, where one can see that there is no significant effect of specimen volume both for longitudinal and transverse directions. In the case of compressive tests on the largest specimens, i. e., those 50 mm in diameter, the initiation and growth of a crack was often observed at the end or side surface of a specimen, being followed by its growth along the longitudinal direction up to fracture. This is probably because some stress concentration took place in the end surface of a specimen in contact with the compression plate. On the other hand the smaller specimens showed clear shear fracture at an angle of about 45 degrees. It is to be noted that despite of the fact above there is no significant dependence of compressive strength on the specimen volume. On the basis of the facts above and general requisite that the specimen size should be at least 10 times larger than the grain size the specimen dimensions shown in Fig. 2 were determined. The digital data on PGX graphite are shown in the Appendix. The diameter and gage length employed here for the fatigue test are twice larger than those of the previous investigation on IG-11 graphite [7].

3.2 Static tensile strength

To evaluate the variance of the tensile strength , the results of tensile tests on fatigue specimens are shown on the normal probability paper for IG-11, PGX and ASR-0RB in Figs. 5, 6 and 7, respectively. The digital data are shown in the Appendix. It is seen in these figures that the distribution of the tensile strength of these materials is well expressed by the normal distribution. The trend was more clearly found for the data set where the more data points taken from several lots of IG-11 and PGX were statistically analyzed [10]. The data on tensile strength also obey the Weibull distribution fairly well, especially at low strength levels.

3.3 Fatigue life at room temperature

Results of the fatigue tests performed in the condition that R=0.0, -1.0 and -3.0 are summarized in the Appendix, Tables A8 through A12 for IG-11, PGX (L)(T) and ASR-0RB (L, T), respectively. In case that a specimen fractured during the first tensile loading in each loading condition, the fatigue life was counted as 0.25 or 0.5 for R=-1 or R=0.

3.3.1 Analysis of data by Price's method

According to Price model the fatigue life N_f is assumed to be expressed as

$$\log (\sigma_a / S_{mean}) = A + B \log N_f + \varepsilon. \qquad (1)$$

Here, σ_a, S_{mean} are the maximum applied stress and the mean tensile strength, respectively. Constants, A and B are determined by the least square method. ε is a normal random variable with the mean value = 0 and the standard deviation = s. In the present analysis specimens with fatigue lives larger than 10^5 were omitted so that the derived equation is considered to be on the conservative side.

The data analyzed on the basis of Eq. (1) are shown in Fig. 8 through 12 for the three materials with several R-values. Digital data for these figures are summarized in the Appendix. In the figures one can see the lines for 99% survival probability with 95% confidence as well as the best fit lines to the data points. Table 2 summarizes values for the parameters A and B with standard deviations in Eq. (1). It is to be noted that the intercept with the ordinate, A and the slope B decrease with decreasing R. All the best fit lines obtained here pass very closely the point (normalized applied stress, fatigue life) = (1.0, 0.25) or (1.0, 0.5), which indicates that the fitness of the equations to the data points is good.

3.3.2 Analysis of data by homologous stress method

Homologous stress is defined as the ratio of the maximum applied stress σ_a to the estimated tensile strength of i-th specimen, S_i, $\sigma_H = \sigma_a/S_i$. S_i is estimated on the assumption that a specimen which displayed the i-th shortest fatigue life in the fatigue specimen set should be the i-th weakest if the static tensile tests are performed on the set of specimens, and that the variations of fatigue life and static strength can be expressed by the normal or Weibull distribution. Here, the homologous stress at each applied stress level was estimated on the basis of these distributions. When the estimation was carried out for the lower applied stress levels, the run-out specimens, i. e., those which had survived up to 10^5 cycles, were regarded to have a fatigue life of 10^5 to minimize the possible error that would be brought about when those specimens would be omitted. There is no large difference in the homologous stress values between the normal and Weibull distributions, although Weibull distribution gave a little larger values at very low fracture probabilities. This is reasonably expected that the fracture probability in the low stress region is the higher for the Weibull than for the normal. However, the difference in the fatigue strength between the two distributions are very small, as is shown in Fig. 13.

Tables 3 and 4 summarizes the values for the parameters in the following equation on the basis of the normal and Weibull distributions, respectively.

$$\log \sigma_H = A + B \log N_f \tag{2}$$

In comparison with the previous calculation , B is a little smaller than that obtained by the Price's method, i. e., the slope is the larger. The values of A are larger than those obtained by Price's method. From these facts it is found that the fatigue strength is much smaller than that in the case of Price's method for all the three materials tested. There is one crucial point about the homologous stress method from the aspect of its application to the design and safety analysis of graphite components : Some homologous stresses become larger than 1.0 when the applied stress level is high. This was also incurred in the previous study on IG-11 graphite [7]. The fact above could be a demerit of the homologous stress method if the method would be used for determining the fatigue life diagram for the design of graphite components. It is also to be noted that the static strength estimated for the analysis depends on the log and heat of the material, the variation within a log, the number of data points, etc.

3.3.3 Analysis by P-S-N diagram method

In the P-S-N diagram method the best fit S-N curve is obtained in the following way : (1) a probability distribution is assumed to the fatigue life at each stress level. (2) the fatigue life at a given fracture probability is estimated for each stress level. (3) plots of the applied stress vs. fatigue life at a given fracture probability are drawn as the best fit S-N curve [10].

Here, the Weibull distribution was assumed to be applicable to the fatigue life at each stress level, i. e.,

$$P_f = 1 - \exp\{-(N_f / N_o)^m\}. \qquad (3)$$

In the above equation, P_f is the cumulative fracture probability at fatigue life N_f, and m, N_o are constants. From Eq. (3),

$$\ln \ln\{1 / (1-P_f)\} = m \ln N_f - m \ln N_o. \qquad (4)$$

Data on IG-11 and PGX graphites were analyzed on the basis of Eq. (4) , which gives Figs. 14 through 16. Data on ASR-0RB was not analyzed by P-T-S method, because the number of specimens tested was not large enough to be analyzed by the method.

P-S-N diagram method is, in principle, to be applied to the data where the fracture probability distribution is the same for all the stress levels, i.e., the m-value in Eq. (4) is the same. However, in reality, as is seen in the figures, the slope decreased with decreasing stress level. Therefore, it is judged that the method is not appropriate for the data analysis on the graphites examined in the present study.

3.3.4 Dependence of S-N curve on R-value

Here, the dependence of the fatigue life on R-value is discussed with regard to S-N curves obtained by Price's method which is believed to be most appropriate to analyze the fatigue data on nuclear graphite. It is to be noted that there is no large difference in A-value between the grades of materials as long as R is the same, i. e., R= 0 or = -1. A-values seem to decrease with decreasing R-value, which is clearly seen in the case of PGX (L) in Table 2. Previous studies on IG-11 graphite indicated that the stress level at N_f= 1 decreased from 0.97 to 0.73 of the mean tensile strength with decreasing R from 0 to -3.5 [7,8]. In the present experiment on PGX graphite (L) the stress level at N_f = 1 is 0.96 of the mean tensile strength at R= -3, much larger than that for IG-11. The stress levels in the compression side in these cases, i. e., R= -3.5 for IG-11 and R= -3.0 for PGX (L), were 0.85 and 0.83 of the mean compressive strength of each material, respectively. The fact indicates that the effect of compressive stress on the fatigue life is more pronounced for IG-11 than for PGX. This is probably because the defects introduced by high compressive stresses propagate less rapidly during the fatigue process for PGX because of its larger grain size and higher deformability. In fact, a previous study on the effect of compressive prestress on the tensile strength of graphite indicates that the fine-grained, higher strength material showed the larger loss in the tensile strength if the normalized prestress level was the same [12].

The absolute value of B increased with increasing R-value. This indicated that the stress in the compression side would affect the growth of the fatigue crack. It is also to be noted that the slope of the S-N curves is less steep for ASR-0RB, comparing with the other materials. This means that practically the fatigue behavior would not be observed in the carbon material when the applied stress level is smaller than 0.8 of the mean tensile strength, probably because of its pronouncedly brittle nature.

3.3.5 Equi-fatigue life diagram

The above discussion indicates that Price's method is the most appropriate to analyze the fatigue data on graphite and carbon materials so that the equi-fatigue life diagram for design, i. e., the modified Goodman diagram, is proposed for PGX and ASR-0RB on the basis of the method. According to the HTTR Graphite Structural Design Code, the design fatigue life curve is to correspond to 99% survival probability with 95% confidence [11]. The design fatigue life curve is given by

$$\log(\sigma_a / S_{mean}) = [\log(\sigma_a / S_{mean})]_{mean} - \left(2.326 + \frac{1.645}{\sqrt{n}}\right) s \qquad (5)$$

Here, $[\log(\sigma_a / S_{mean})]_{mean}$ represents the stress value of the best fit curve, and n is the number of data points, s, the standard deviation defined in Eq. (1). The design curves for N_f =1, 10^3 and 10^5 are shown in Figs. 17 and 18 for PGX and ASR-0RB, respectively. In these figures, the mean applied stress is assumed to be equal to the mean tensile strength for the case R= 1.

3.4 Fatigue life at high temperature

3.4.1 Tensile strength of IG-11 graphite

Results of the tensile test on high temperature fatigue specimen with different treatments are summarized in Table 5. It is to be noted that the tensile strength at room temperature in vacuo is about 24% larger than that in air. This trend was also observed in the previous experiment [13] where the tensile strength was found to be about 15% larger in vacuo than in air at room temperature. Though, in the present study, it is rather difficult to evaluate quantitatively the effect of atmosphere on the strength, it is believed that the service condition of the HTTR would increase the strength of the graphite in comparison with that in air. It is also interesting to see that the heat treatment at 200℃ in vacuo for 2h increased the strength at room temperature by a few %, resulting in the strength value which coincides with that at 980℃. The strength of specimens which survived after more than 10^5 cycles of repeated applied stress seem to have kept the original strength, comparable with or even larger than that obtained at room temperature in vacuo. From these results it was decided that the mean tensile strength to be used in the normalization of the applied stress in the high temperature fatigue test was either that at room temperature in vacuo or that at 980℃ in vacuo, i. e., 40.3 MPa or 42.8 MPa, and the analysis of the fatigue data was done for both cases.

3.4.2 Fatigue strength at 980℃

The results of the fatigue test at 980℃ are shown in Fig. 19 (a), (b) where one can see the plots of the normalized applied stress versus fatigue life in comparison with the best fit equation for the room temperature data obtained in the previous study [8]. In Fig.19 (a) the applied stress is normalized to the mean tensile strength at 980℃ whereas the mean strength at room temperature in vacuo is chosen as the normalizing strength in Fig. 19 (b). The best fit line in the latter case is expressed as

$$\log (\sigma_a / S_{mean}) = - 0.0166 - 0.00770 \log N_f \qquad (6)$$

which is very close to that obtained for the room temperature fatigue strength in the condition of R= 0 [8], i. e.,

$$\log (\sigma_a / S_{mean}) = - 0.0136 - 0.00877 \log N_f \qquad (7)$$

On the other hand, the fatigue strength appears to be rather low if the normalizing strength is set at the mean strength at 980℃ in vacuo, i. e.,

$$\log (\sigma_a / S_{mean}) = - 0.0427 - 0.00776 \log N_f \qquad (8)$$

The value of σ_a / S_{mean} at 10^5 cycles is 0.881 and 0.829 for Eqs. (6) and (8), respectively. For the room temperature fatigue strength, σ_a / S_{mean} is 0.876. From the above calculations it is concluded that the fatigue strength at 980℃ is well described by an equation analogous to that for the room temperature fatigue strength when the mean strength at room temperature is chosen as the normalizing strength. If the normalizing strength is set at the mean strength at 980℃, the best fit line gives the lower fatigue strength than is estimated from the data on the room temperature fatigue strength. This implies that the fatigue strength at 980℃ is evaluated on the conservative side if the applied stress is normalized to the mean tensile strength at 980℃. One thing to be noted is that 17 out of 38 specimens which were subject to repeated stresses survived even at 10^5 or more, and that the fatigue life of these specimens was treated as 10^5 in the present analysis. The fact is believed to make the analysis even more conservative.

4. Conclusions

Room temperature fatigue tests were carried out on PGX graphite, ASR-0RB carbon and IG-11 graphite which are used in the core region of the HTTR. The ratio of applied stress $R= \sigma_{min} / \sigma_{max}$ was -3, -1, 0 (PGX), -1, 0 (ASR-0RB) and -1 (IG-11). The room temperature data were analyzed by three different methods, i. e., Price's, homologous stress and P-T-S diagram to investigate which method is the most appropriate. Fatigue tests were also carried out at 980℃ in vacuo for IG-11 graphite to evaluate the effect of temperature on the fatigue strength.

Main conclusions are :

1) Among the three methods above the Price's method was the most appropriate to derive a design S-N curve from the data set. P-T-S diagram method could not be applied to the present data.
2) The fatigue strength of PGX and ASR-0RB decreased with decreasing R-value, which is consistent with the result which was obtained previously on IG-11. Although the variation of data was the largest among three materials, the fatigue strength normalized to the mean tensile strength was the largest for ASR-0RB.
3) On the basis of the room temperature data analyzed by Price's method, design S-N curves were obtained for PGX and ASR-0RB.
4) Fatigue tests at 980℃ on IG-11 graphite indicated that the S-N curve was almost the same as that for the room temperature curve when the applied stress was normalized to the mean tensile strength at room temperature in vacuo.

Acknowledgments

The authors are indebted to Messrs, M. Matsumoto and S. Sawahata for the high temperature fatigue test. They are also grateful to Dr. T. Iyoku for valuable comments.

References

1. T. Arai, et al., JAERI-M 86-192 (1986), p. 58
2. R. Vollman, et al., ibid., p.43.
3. T. Iyoku et al., ibid., p120.
4. HTTR Design Laboratory, JAERI-M 89-006 (1989).
5. R. J. Price, Carbon 16, 367 (1978).
6. J. B. S. Wilkins and A. R. Rice, AECL-4216 (1972).
7. S. Ishiyama and T. Oku, JAERI-M 86-145 (1986).
8. S. Ishiyama et al., J. At. Soc. of Japan 29, 651 (1987).
9. M. Eto et al., JAERI-M 84-148 (1984).
10. J. Soc. for Mechanical Engineers, JSME S002 (1981).
11. HTTR Design Laboratory, JAERI-M 89-006 (1989).
12. T. Oku and M. Eto, Carbon 11, 639 (1973).
13. M. Eto et al., Carbon 29, 11 (1990).

Table 1 Some mechanical properties of specimens used in the present experiment

Grade	Direction	Apparent density (g/cm^3)	Young's modulus (GPa)	Tensile strength (MPa)	Bending strength (MPa)	Compressive strength (MPa)
IG-11	L	1.78	10.12	27.83	40.51	80.91
PGX	L	1.74	6.61	8.29	10.91	30.59
	T	1.74	8.49	9.18	11.61	30.24
ASR-0RB	L	1.65	9.45	6.51	11.37	57.95
	T	1.65	10.72	6.78	11.91	50.39

L : Parallel to the longitudinal axis of the block

T : Perpendicular to the longitudinal axis of the block

Table 2 Results of statistical fatigue data analysis by Price method

Grade	Direction	Stress ratio, R $\frac{\sigma_{min}}{\sigma_{max}}$	Intercept of least squares line, A	Slope of least squares line, B	Standard deviation s	Normalized stress for survival to 10^5 cycle $\frac{\sigma_{max}}{S_{mean}}$	
						50% probability	99/95 lower tolerance limit
IG-11	L	-1	-0.0072	-0.0235	0.0199	0.750	0.668
PGX	L	0	-0.0058	-0.0098	0.0293	0.881	0.744
		-1	-0.0092	-0.0215	0.0330	0.765	0.632
		-3	-0.0195	-0.0360	0.0323	0.632	0.524
	T	0	-0.0094	-0.0133	0.0228	0.840	0.736
		-1	-0.0100	-0.0230	0.0257	0.750	0.646
ASR-ORB	L	0	-0.0046	-0.0073	0.0291	0.910	0.766
		-1	-0.0096	-0.0078	0.0304	0.894	0.747
	T	0	-0.0057	-0.0054	0.0370	0.927	0.745
		-1	-0.0097	-0.0138	0.0385	0.835	0.664

Table 3 Results of statistical fatigue data analysis by homologous stress method (Normal distribution)

Grade	Direction	Stress ratio, R $\frac{\sigma_{min}}{\sigma_{max}}$	Intercept of least squares line, A	Slope of least squares line, B	Homologous stress limit, $\frac{\sigma_{max}}{S_{mean}}$ for survival to 10^5 cycles 50% probability
IG-11	L	-1	0.0206	-0.0319	0.661
PGX	L	0	0.0299	-0.0253	0.698
		-1	0.0448	-0.0428	0.551
		-3	0.0060	-0.0432	0.600
	T	0	0.0077	-0.0227	0.756
		-1	0.0228	-0.0354	0.632

Table 4 Results of statistical fatigue data analysis by homologous stress method (Weibull distribution)

Grade	Direction	Stress ratio, R $\frac{\sigma_{min}}{\sigma_{max}}$	Intercept of least squares line, A	Slope of least squares line, B	Homologous stress limit, $\frac{\sigma_{max}}{S_{mean}}$ for survival to 10^5 cycles 50% probability
IG-11	L	-1	0.0214	-0.0322	0.657
PGX	L	0	0.0312	-0.0262	0.688
		-1	0.0473	-0.0438	0.542
		-3	0.0051	-0.0433	0.600
	T	0	0.0098	-0.0233	0.748
		-1	0.0248	-0.0360	0.624

Table 5 Tensile strength of IG-11 graphite in different test conditions

Condition	Tensile strength (MPa)
980℃ in vacuo	42.8 ± 2.0 (8)
RT in vacuo	40.3 ± 3.7 (3)
RT in vacuo after > 10^5 cycles	40.9 ± 1.4 (17)
RT in vacuo after 200℃×2h	42.8 ± 0.7 (4)
RT in air (including after > 10^5)	32.4 ± 2.3 (3)

( ) : Number of specimen

Table 6 Fatigue life of IG-11 (L) at 980℃ in comparison with that at room temperature (R= 0)

Temperature	Stress normalization	A	B
RT	Applied stress normalized to the mean tensile strength at room temperature in air.	-0.0136	-0.00877
980℃	Applied stress normalized to the mean tensile strength at 980℃.	-0.0427	-0.00776
980℃	Applied stress normalized to the mean tensile strength at room temperature.	-0.0166	-0.00770

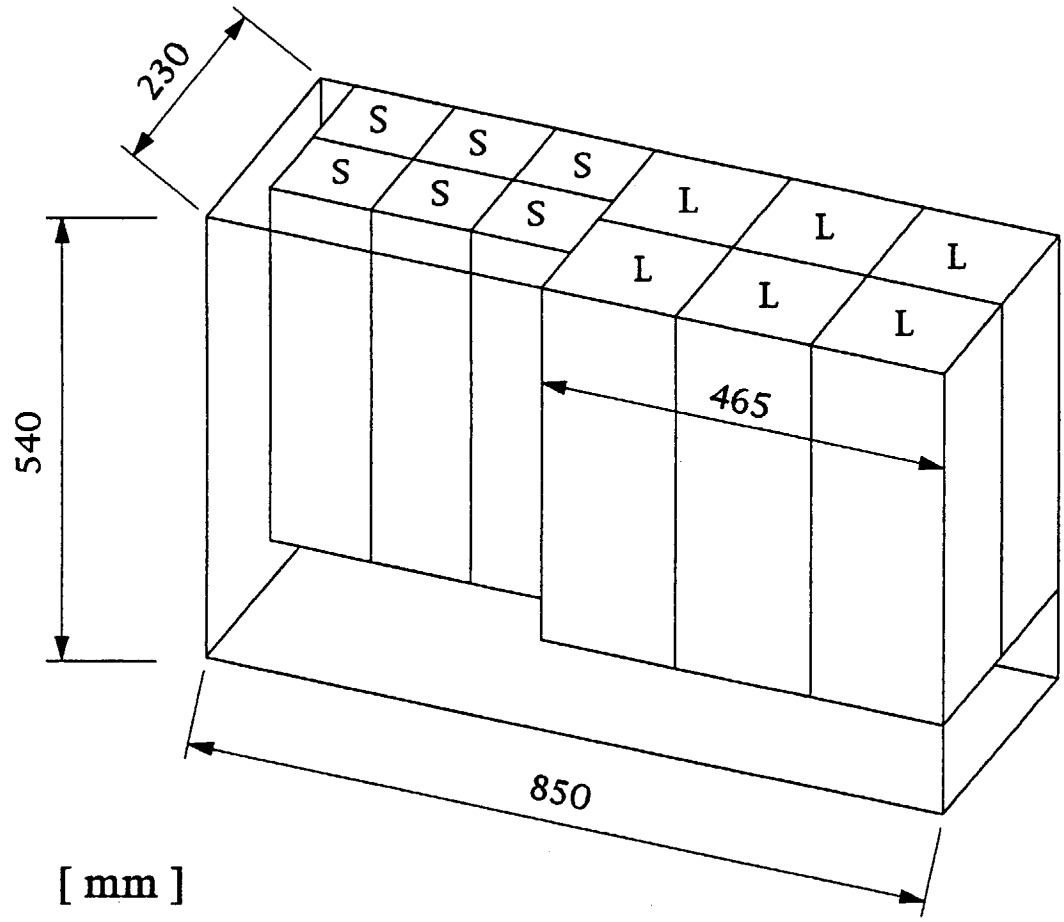

Size of the blocks : Large (L) : 155$^{\square}$×500 mm Small (S) : 115$^{\square}$×430 mm

Fig. 1 Size of the original block and cutting plan for specimen preparation for IG-11 graphite.

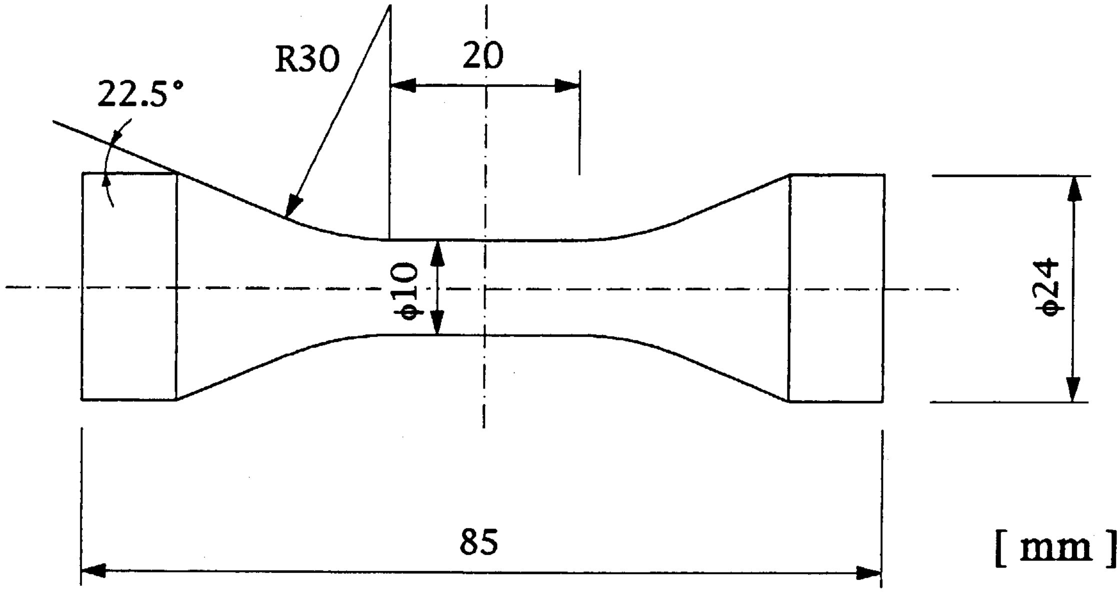

Fig. 2 Specimen for the room temperature fatigue test.

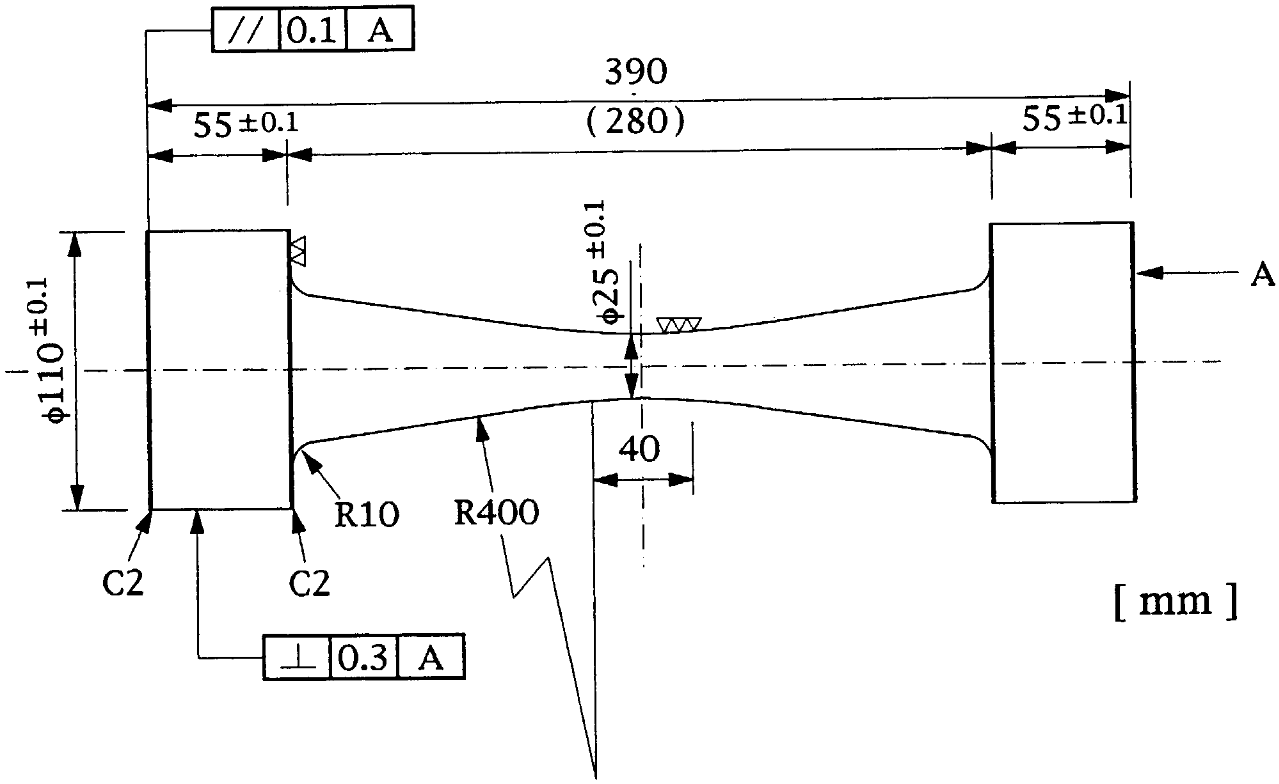

Fig. 3 Specimen for the high temperature fatigue tests.

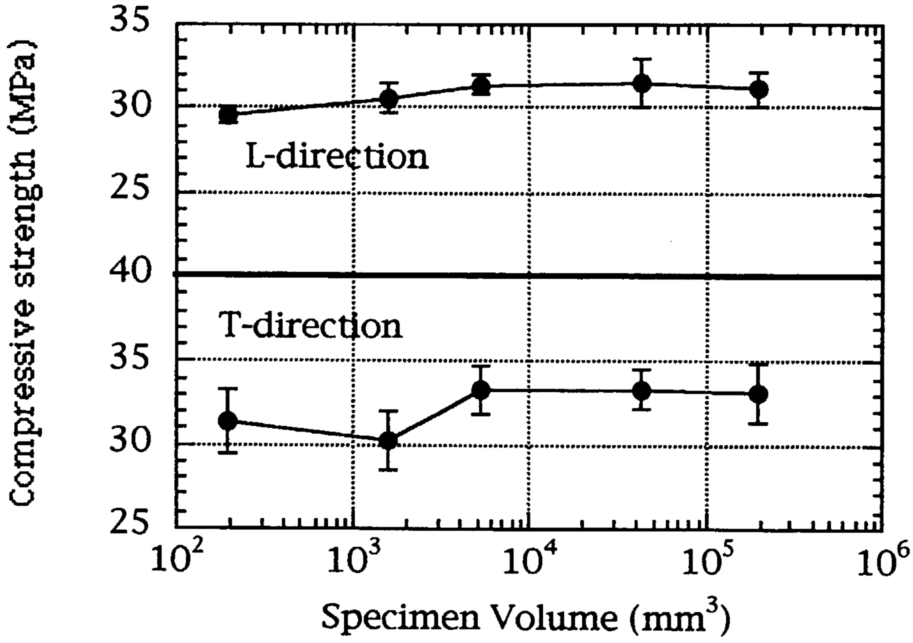

Fig.4 (a)

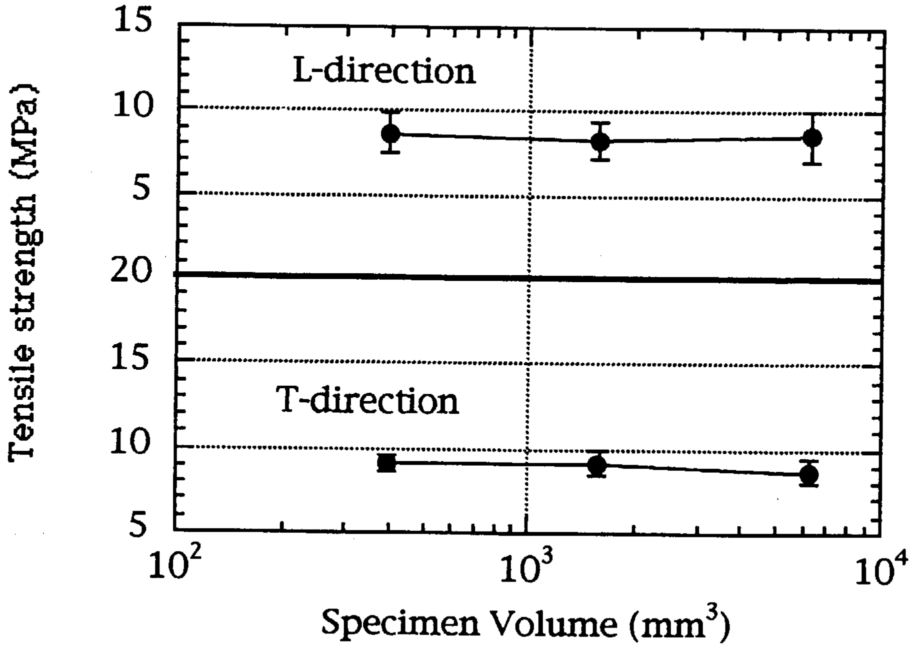

Fig.4 (b)

Fig. 4 Tensile and compressive strength of PGX graphite specimens with different volumes. (a) tensile strength, (b) compressive strength.

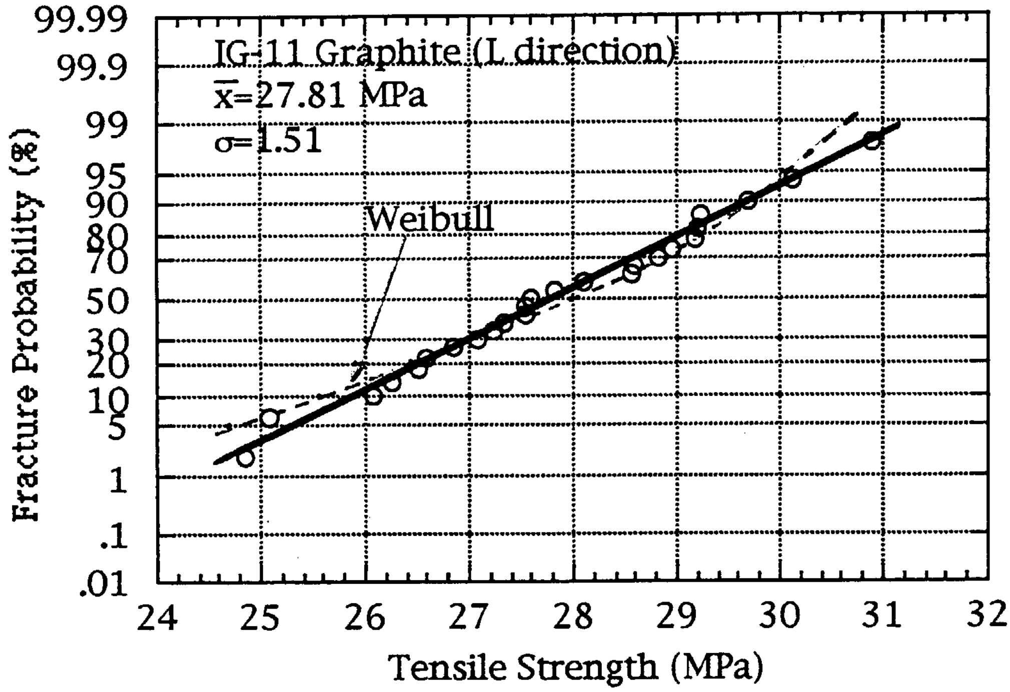

Fig. 5 Plots of fracture probability versus tensile strength of IG-11 graphite specimens (L-direction).

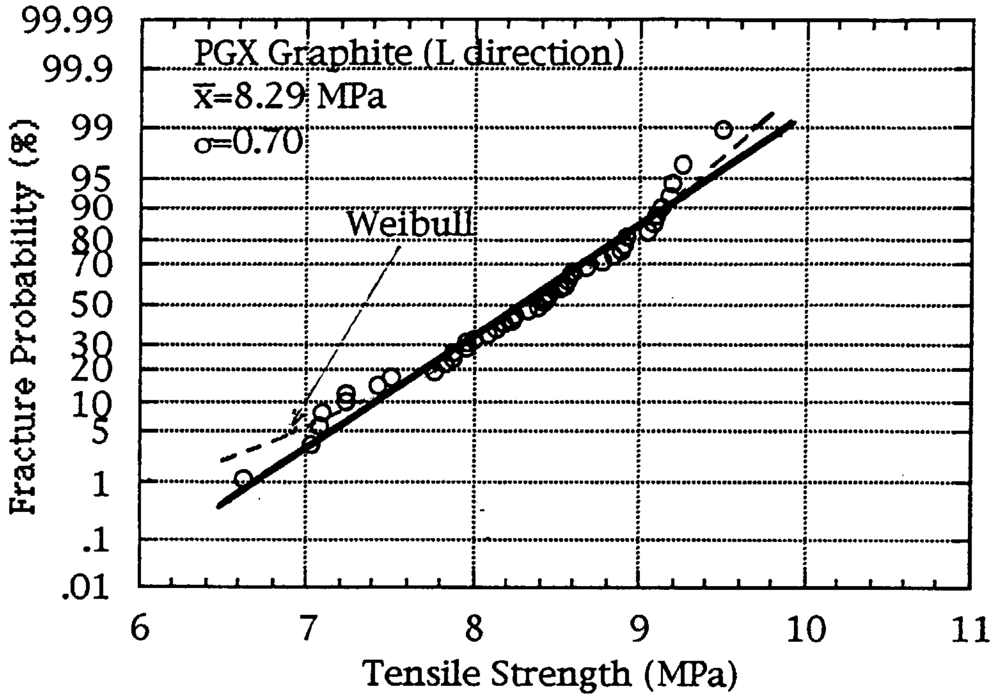

Fig. 6(a)

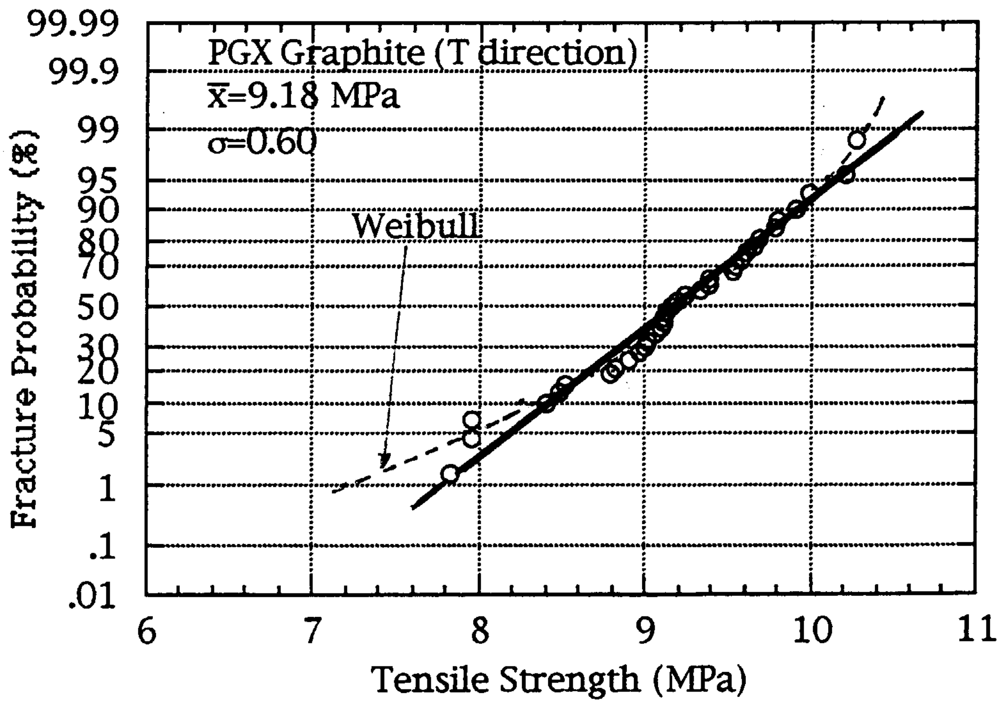

Fig. 6(b)

Fig. 6 Plots of fracture probability versus tensile strength of PGX graphite specimens, (a) L-direction and (b) T-direction.

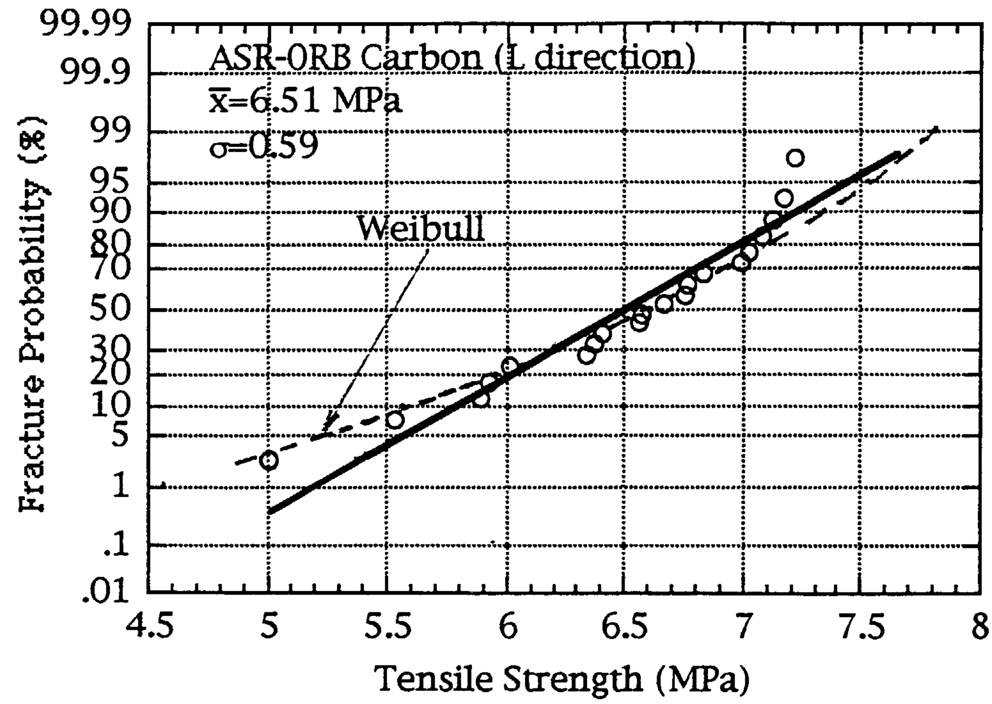

Fig. 7(a)

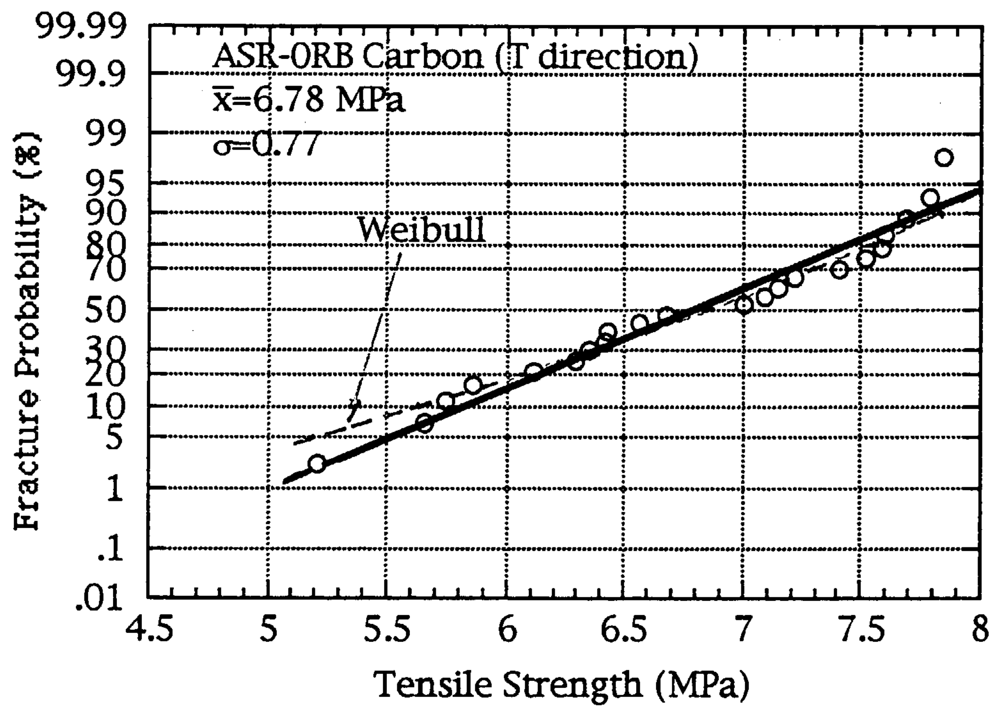

Fig. 7(b)

Fig. 7 Plots of fracture probability versus tensile strength of ASR-0RB carbon specimens, (a) L-direction and (b) T-direction.

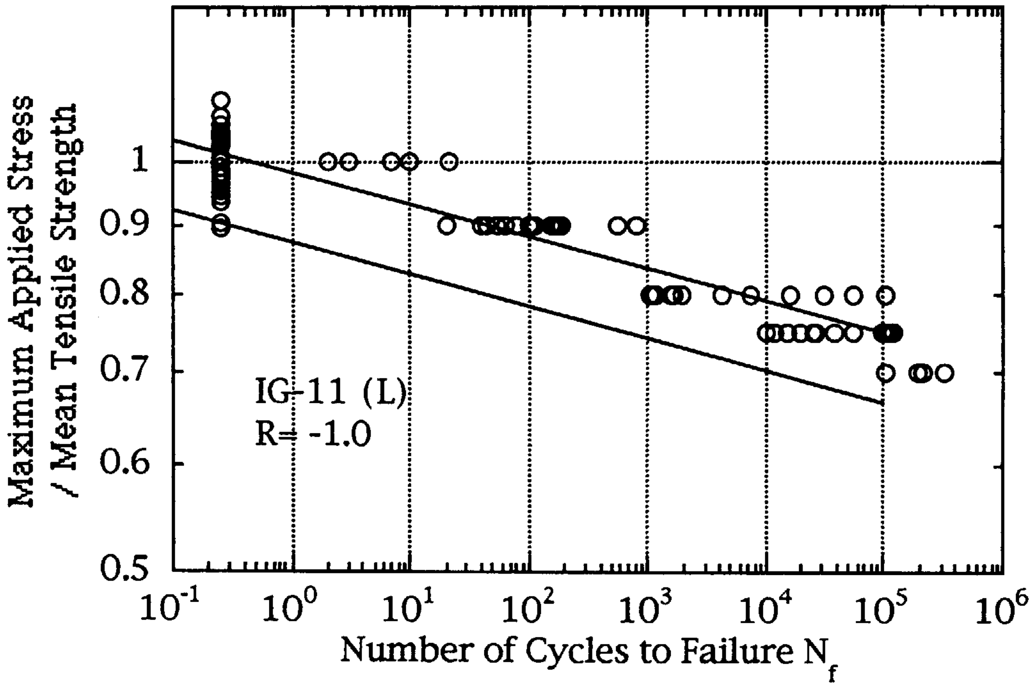

Fig. 8 Fatigue test data with R=-1.0 on IG-11 graphite (L-direction), the S-N curves obtained by Price method. A 99/95% lower tolerance limit represents the limit above which at least 99% of all data would fall with 95% confidence.

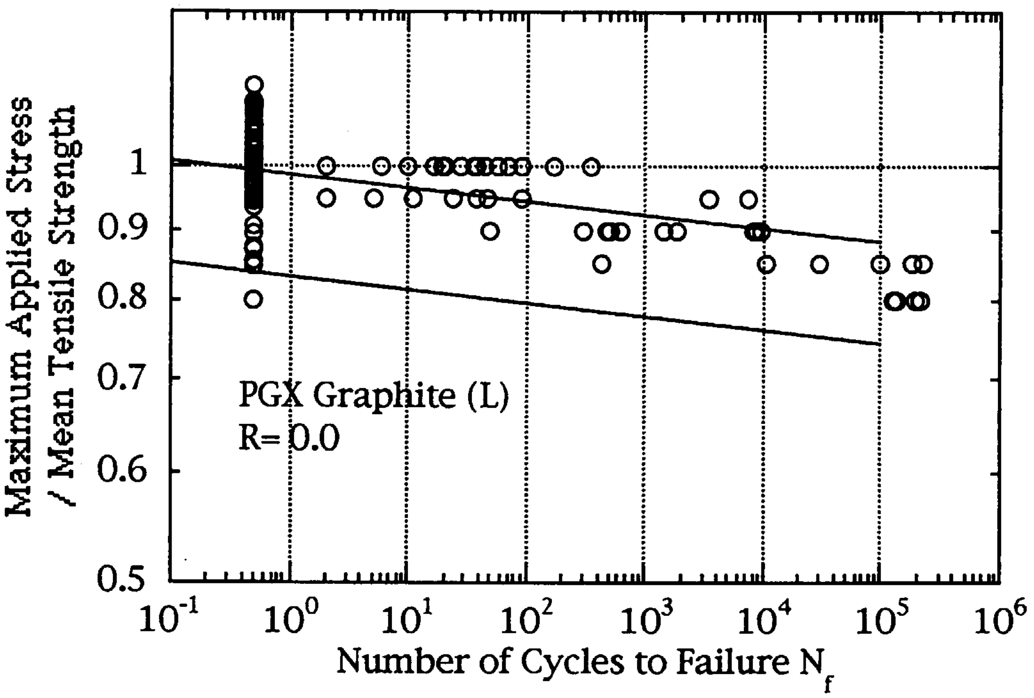

Fig. 9(a) Fatigue test data with R=0.0 on PGX graphite (L-direction), the S-N curves obtained by Price method. A 99/95% lower tolerance limit represents the limit above which at least 99% of all data would fall with 95% confidence.

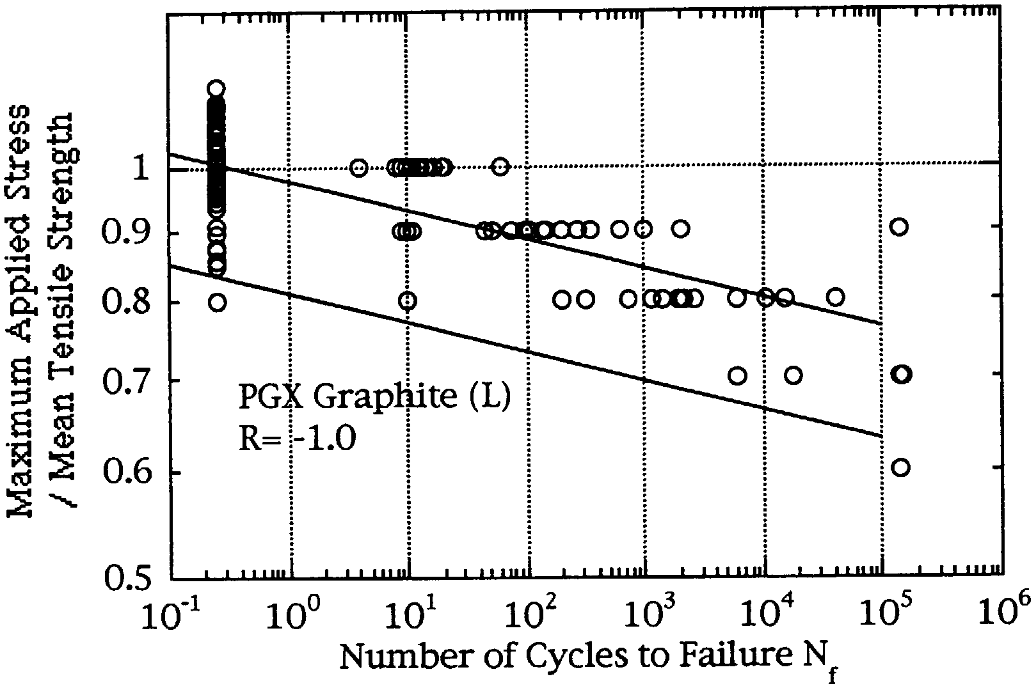

Fig. 9(b) Fatigue test data with R=-1.0 on PGX graphite (L-direction), the S-N curves obtained by Price method. A 99/95% lower tolerance limit represents the limit above which at least 99% of all data would fall with 95% confidence.

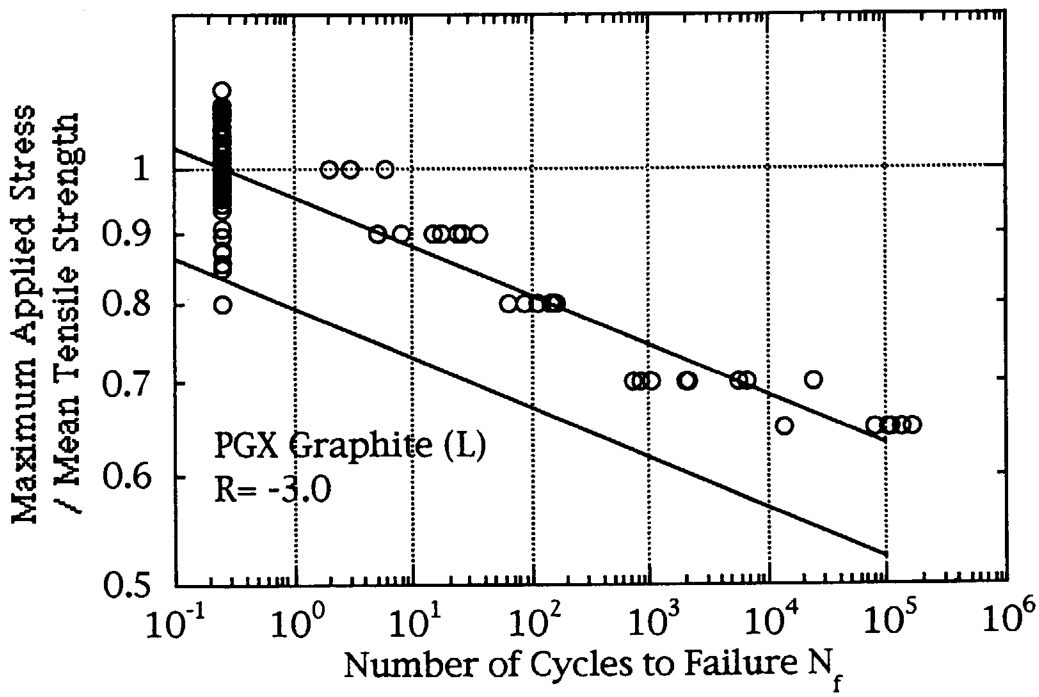

Fig. 9(c) Fatigue test data with R=-3.0 on PGX graphite (L-direction), the S-N curves obtained by Price method. A 99/95% lower tolerance limit represents the limit above which at least 99% of all data would fall with 95% confidence.

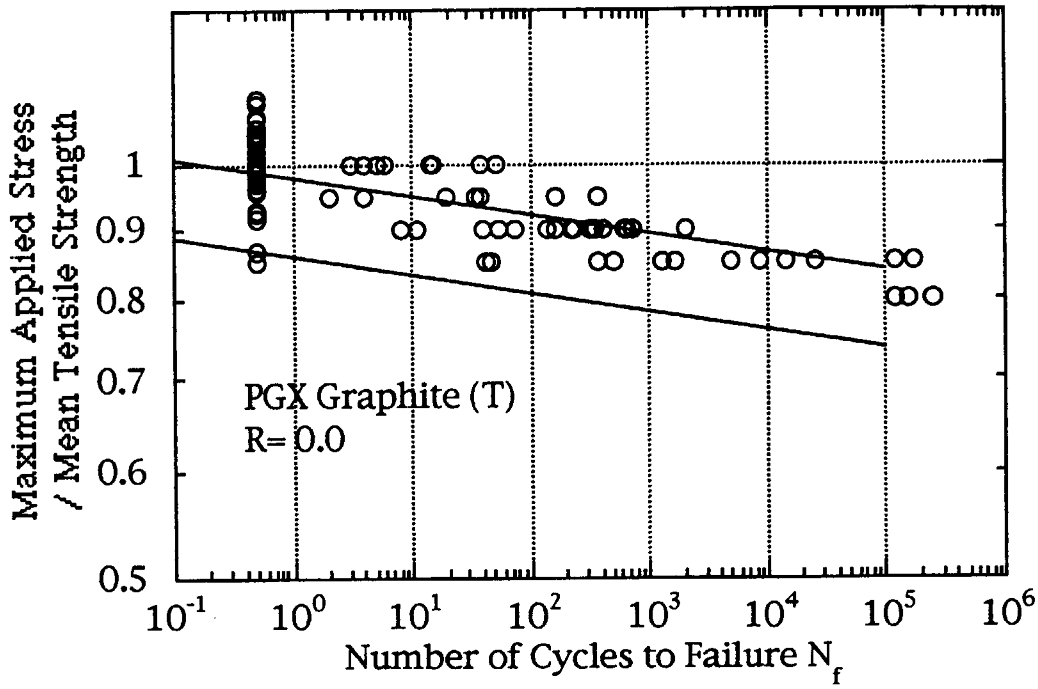

Fig.10(a) Fatigue test data with R=0.0 on PGX graphite (T-direction), the S-N curves obtained by Price method. A 99/95% lower tolerance limit represents the limit above which at least 99% of all data would fall with 95% confidence.

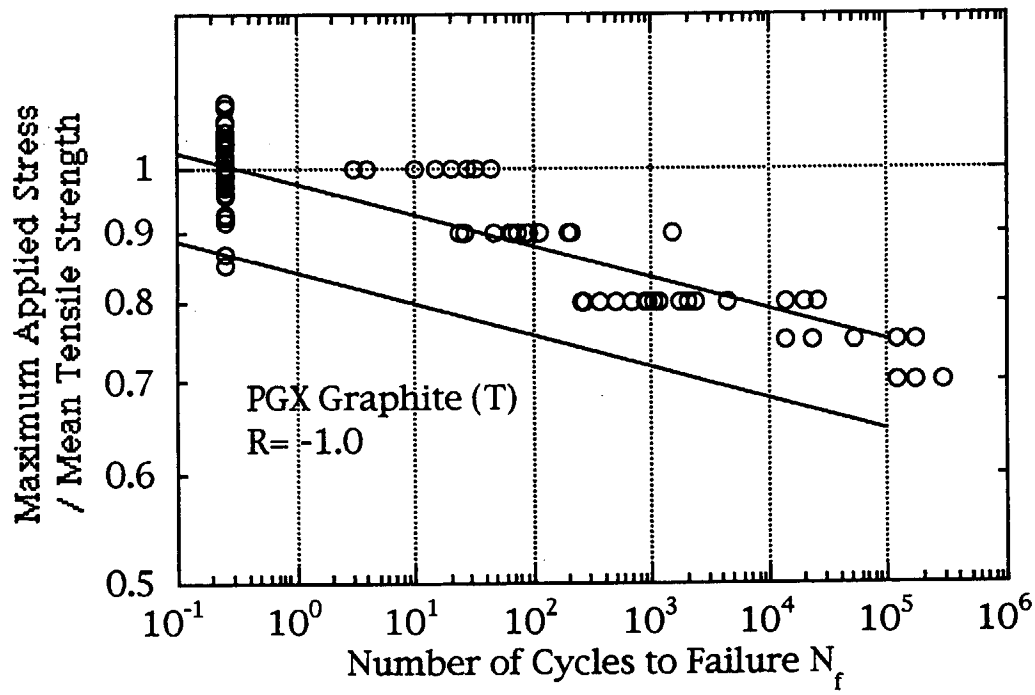

Fig.10(b) Fatigue test data with R=-1.0 on PGX graphite (T-direction), the S-N curves obtained by Price method. A 99/95% lower tolerance limit represents the limit above which at least 99% of all data would fall with 95% confidence.

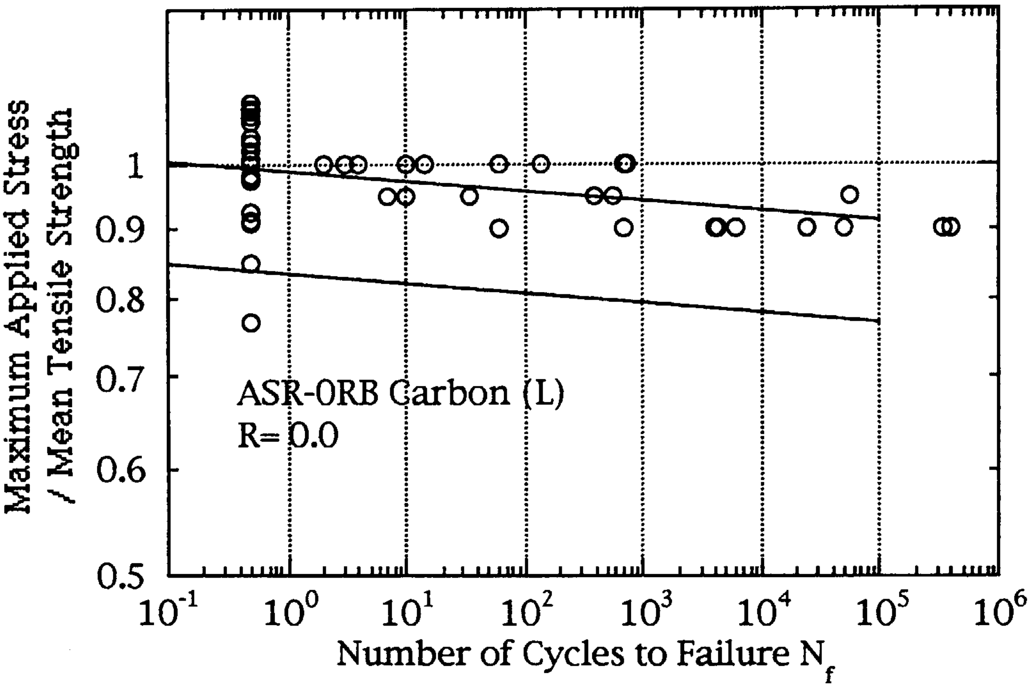

Fig.11(a) Fatigue test data with R=0.0 on ASR-0RB carbon (L-direction), the S-N curves obtained by Price method. A 99/95% lower tolerance limit represents the limit above which at least 99% of all data would fall with 95% confidence.

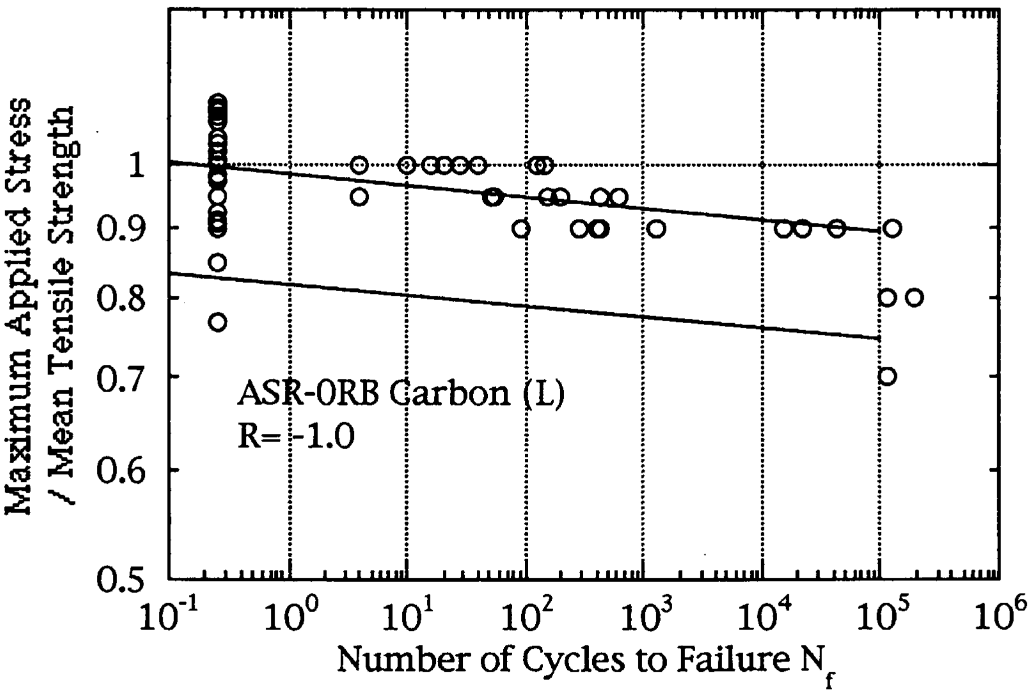

Fig.11(b) Fatigue test data with R=-1.0 on ASR-0RB carbon (L-direction), the S-N curves obtained by Price method. A 99/95% lower tolerance limit represents the limit above which at least 99% of all data would fall with 95% confidence.

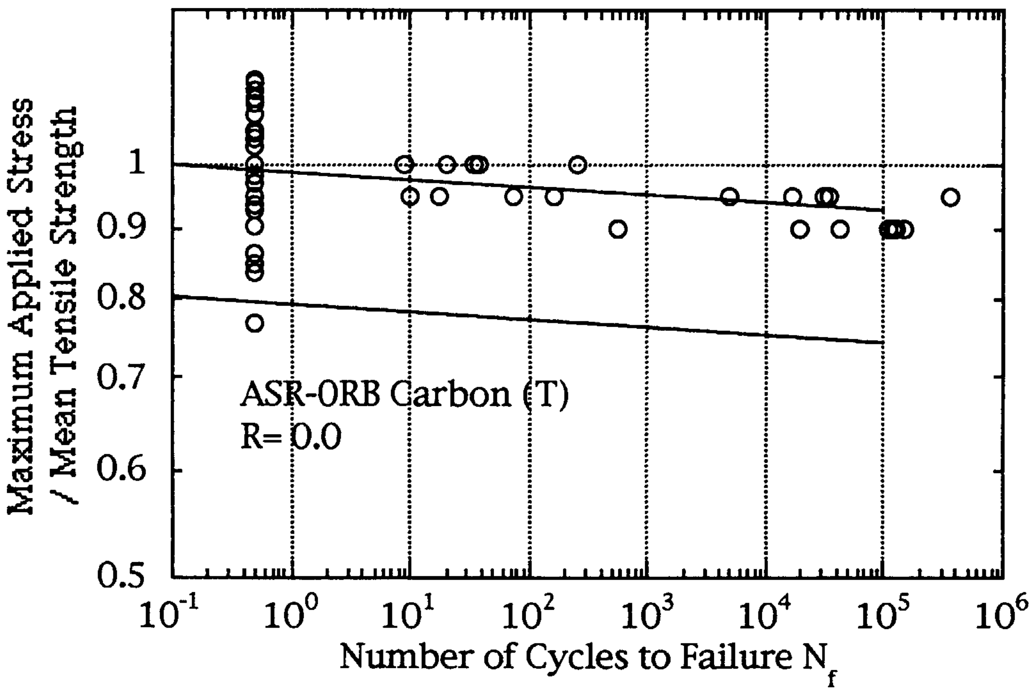

Fig.12(a) Fatigue test data with R=0.0 on ASR-ORB carbon (T-direction), the S-N curves obtained by Price method. A 99/95% lower tolerance limit represents the limit above which at least 99% of all data would fall with 95% confidence.

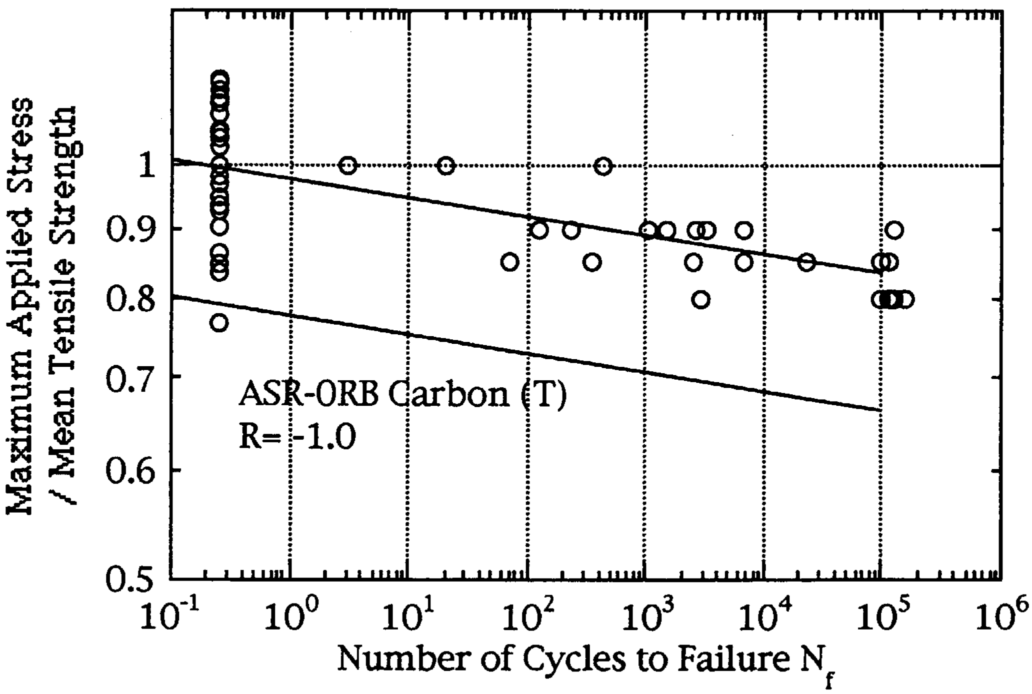

Fig.12(b) Fatigue test data with R=-1.0 on ASR-ORB carbon (T-direction), the S-N curves obtained by Price method. A 99/95% lower tolerance limit represents the limit above which at least 99% of all data would fall with 95% confidence.

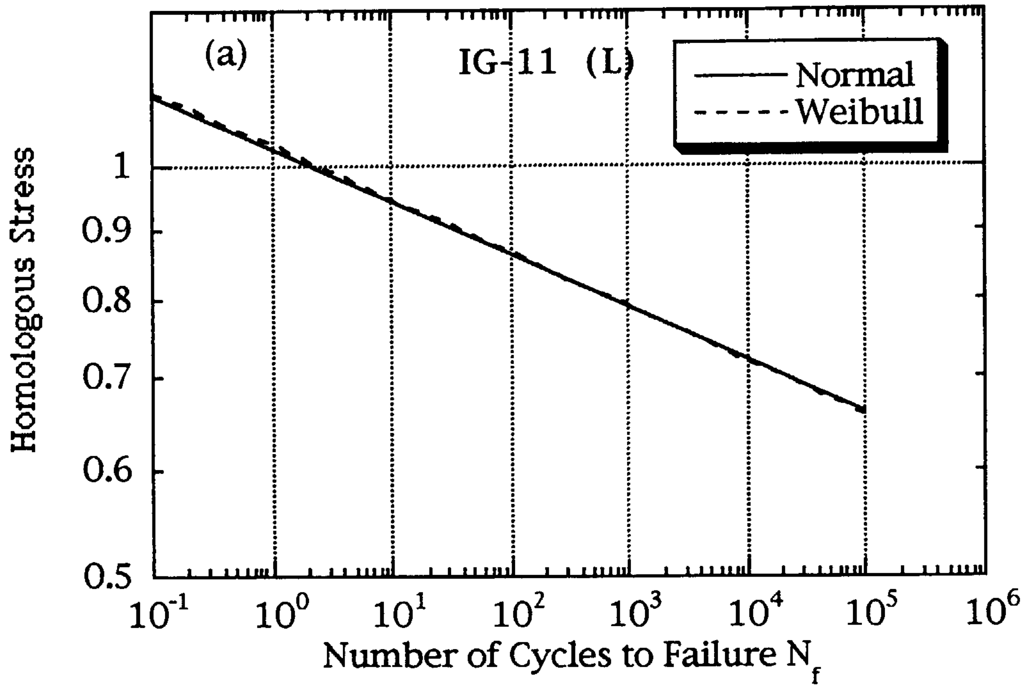

Fig.13 Analysis by the homologous stress method: comparison of the best fit lines on the basis of the normal and Weibull distribution.
(a) IG-11 (L), R= -1,

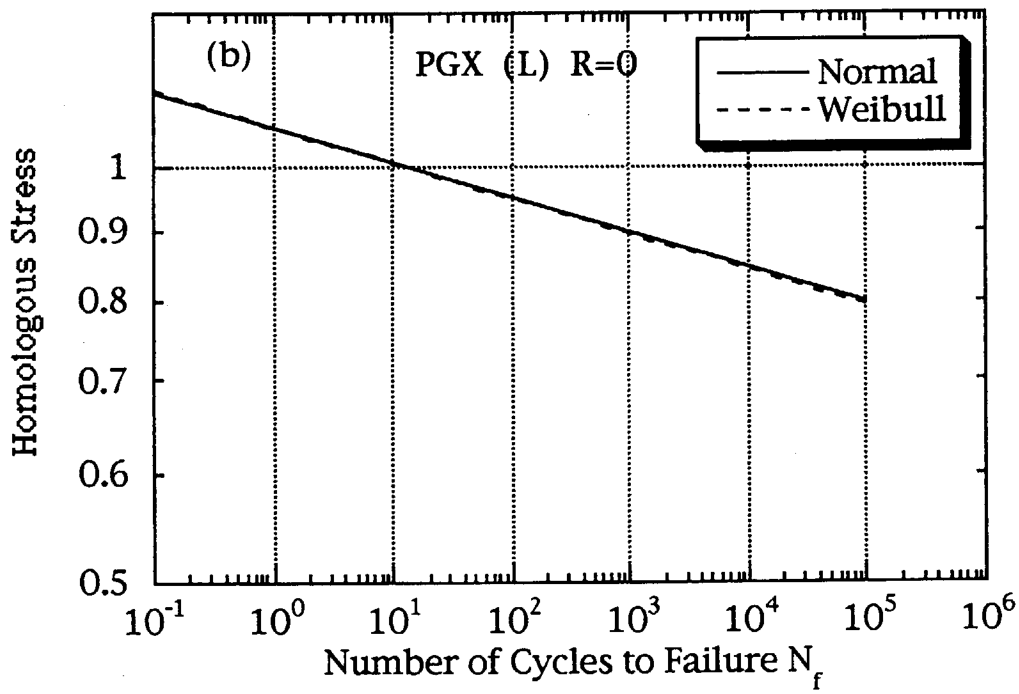

(b) PGX (L), R= 0,

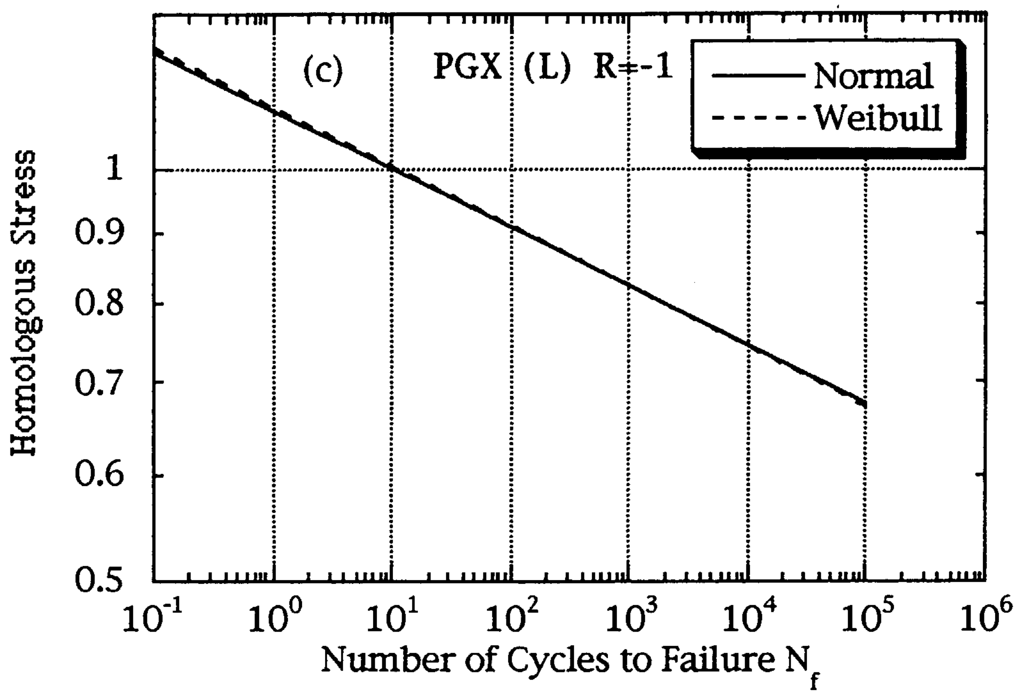

(c) PGX (L), R= -1,

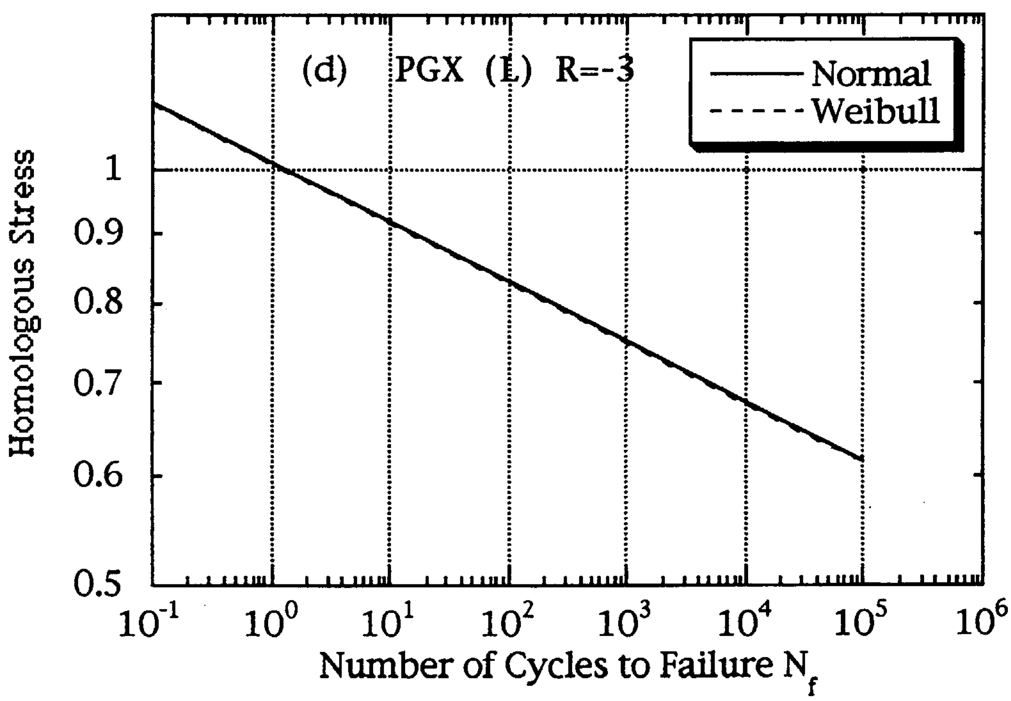

(d) PGX, (L), R= -3,

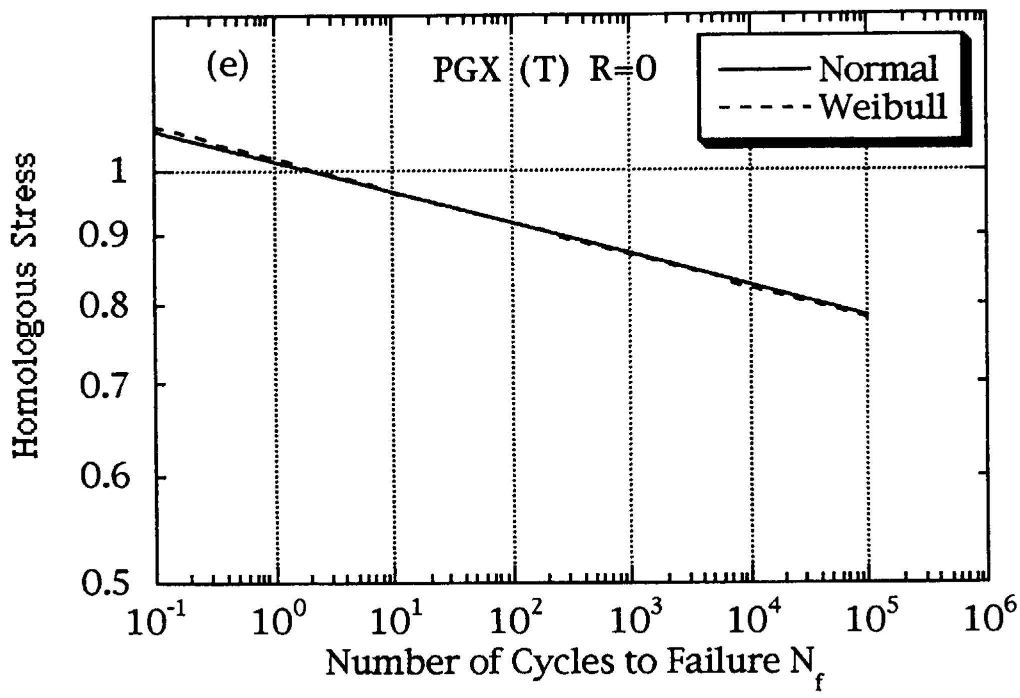

(e) PGX (T), R= 0,

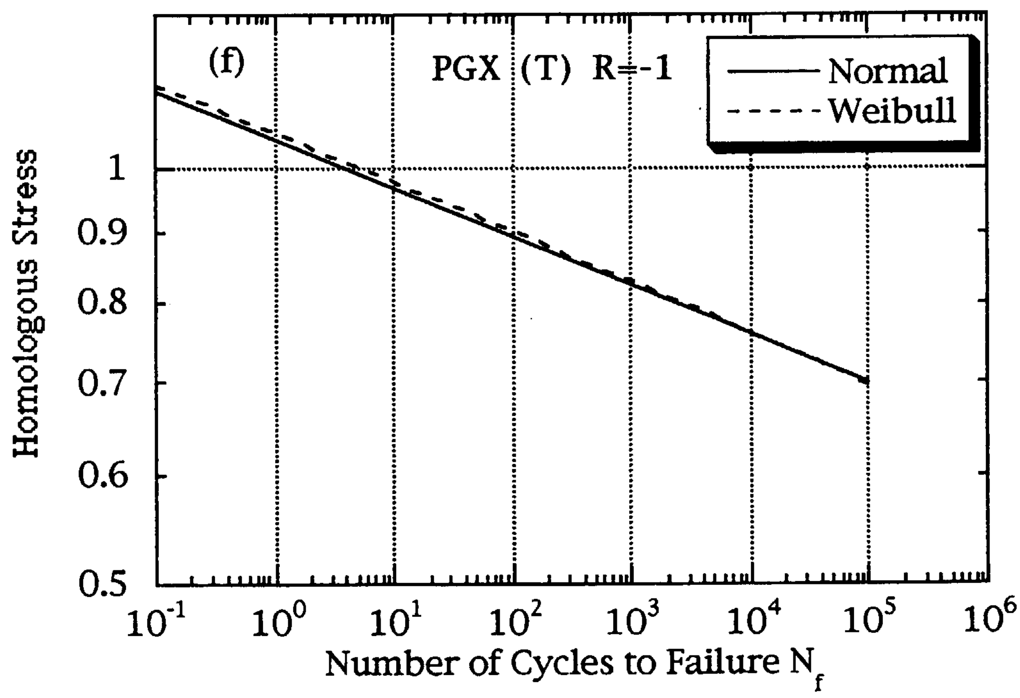

(f) PGX (T), R= -1.

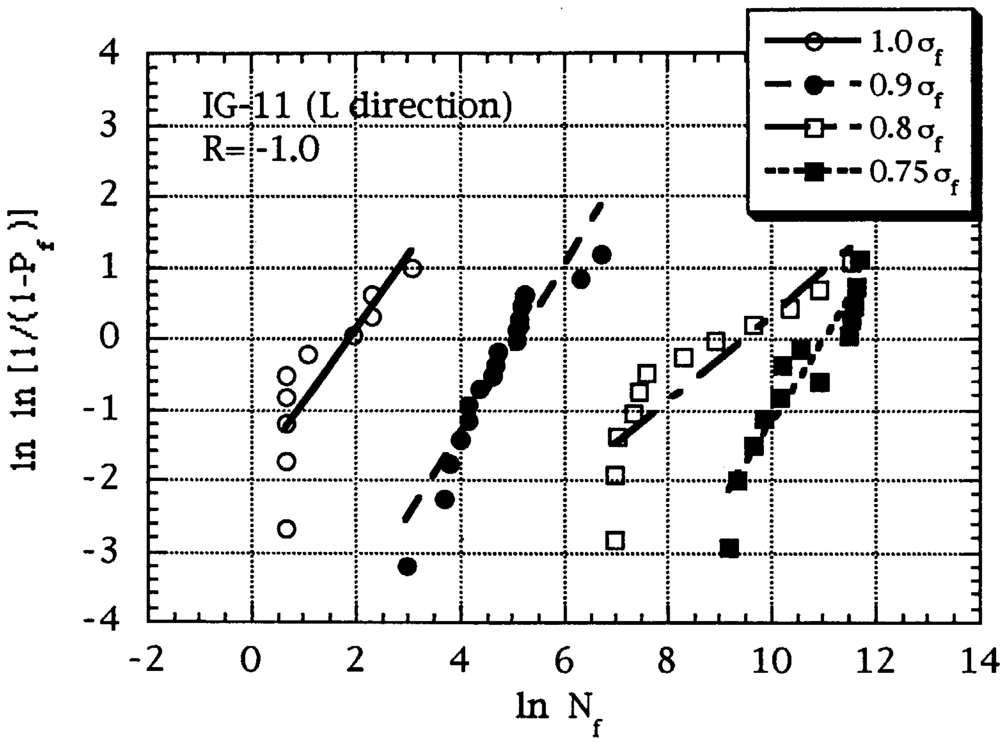

Fig.14 Plot of fatigue test data with R=-1.0 on IG-11 graphite (L-direction) for P-S-N analysis.

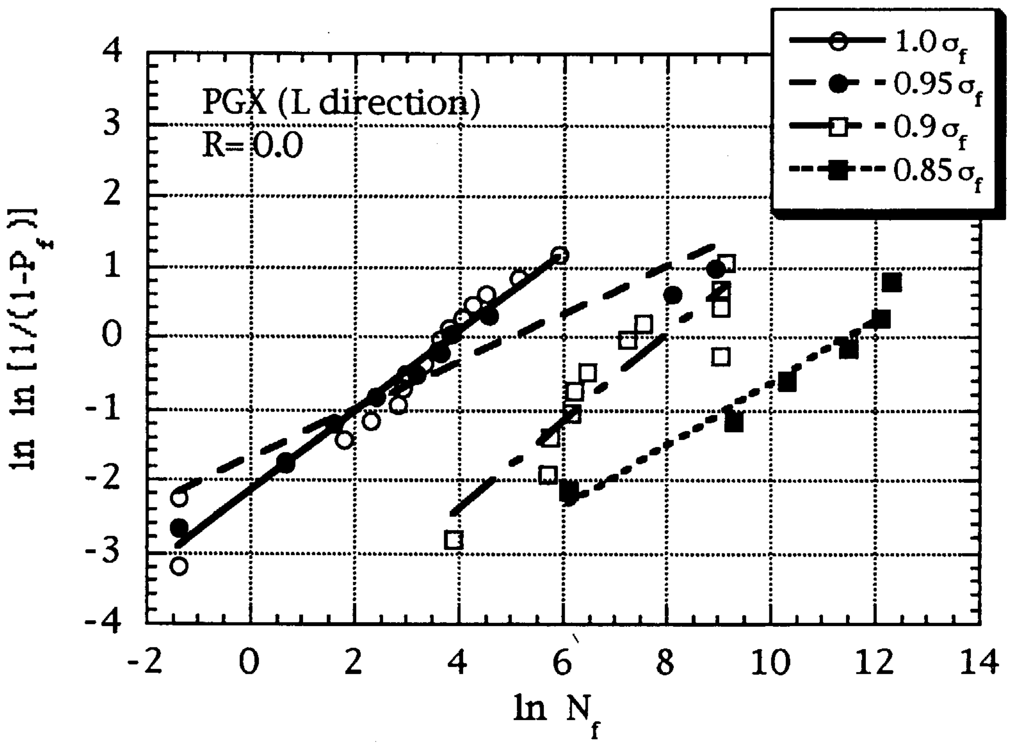

Fig.15(a) Plot of fatigue test data with R=0.0 on PGX graphite (L-direction) for P-S-N analysis.

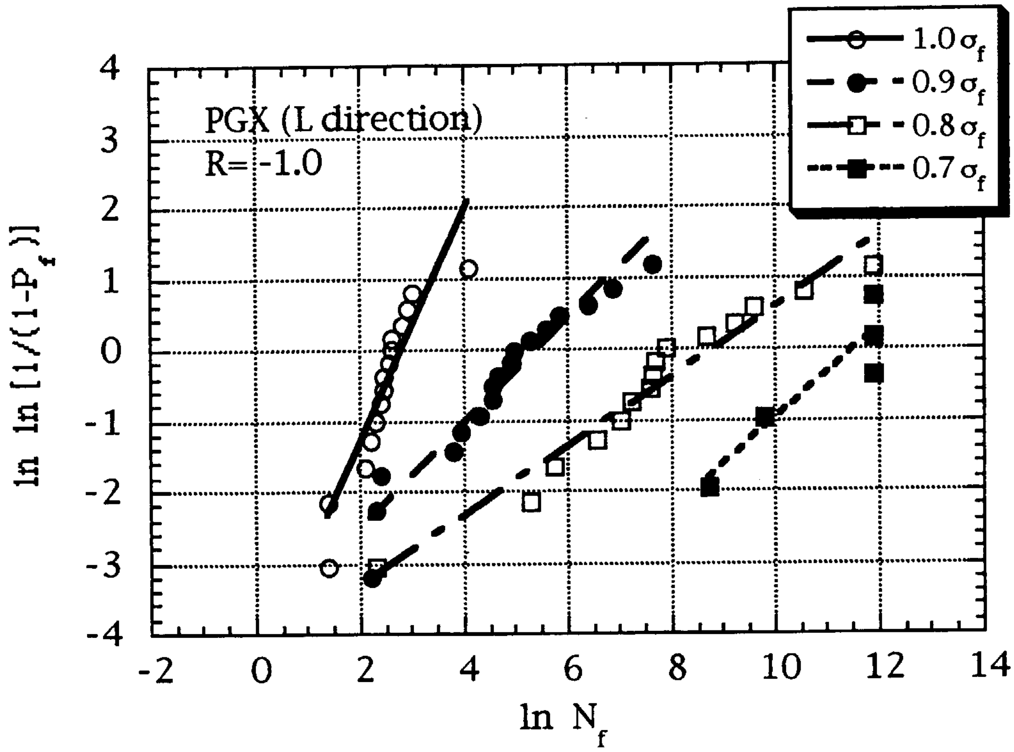

Fig.15(b) Plot of fatigue test data with R=-1.0 on PGX graphite (L-direction) for P-S-N analysis.

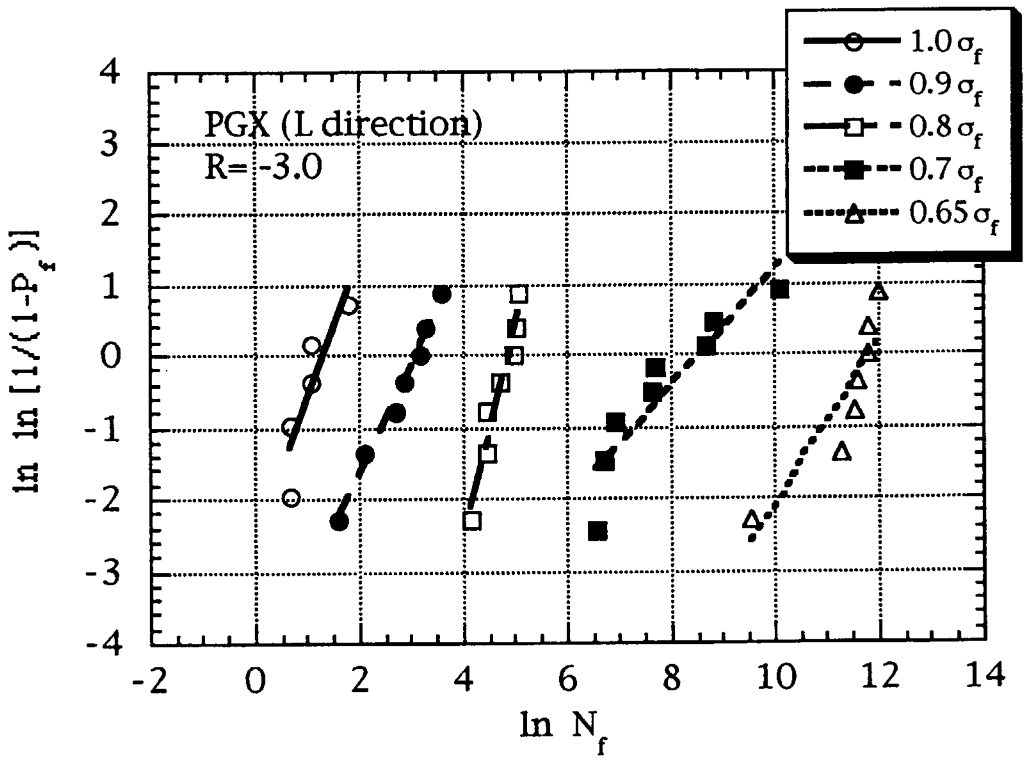

Fig.15(c) Plot of fatigue test data with R=-3.0 on PGX graphite (L-direction) for P-S-N analysis.

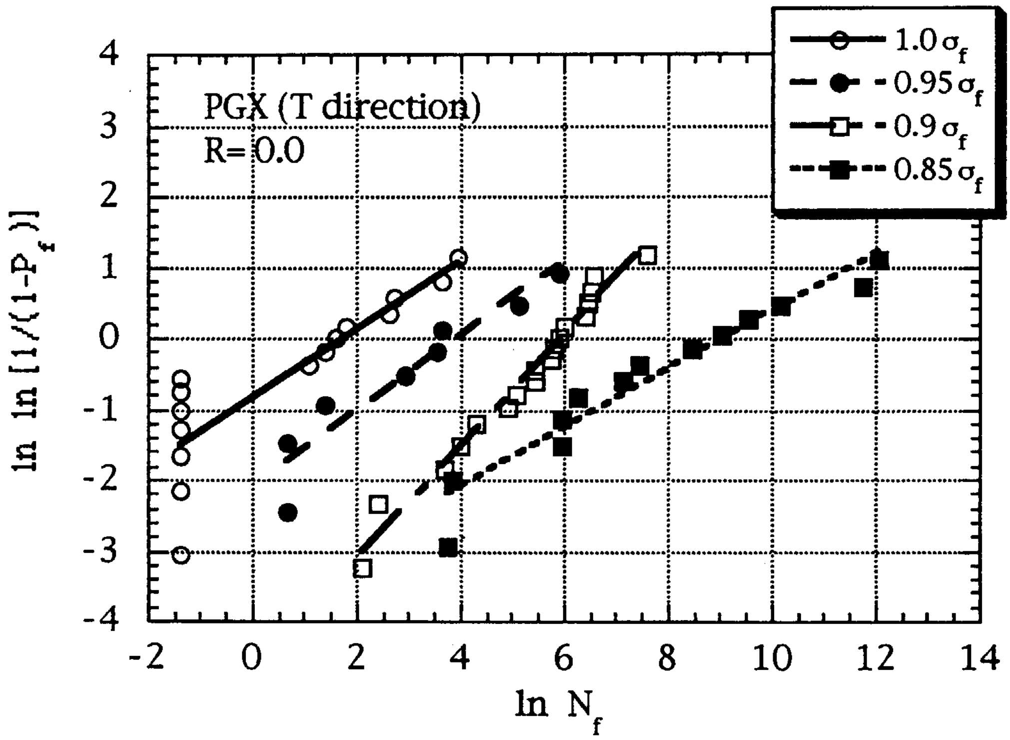

Fig.16(a) Plot of fatigue test data with R=0.0 on PGX graphite (T-direction) for P-S-N analysis.

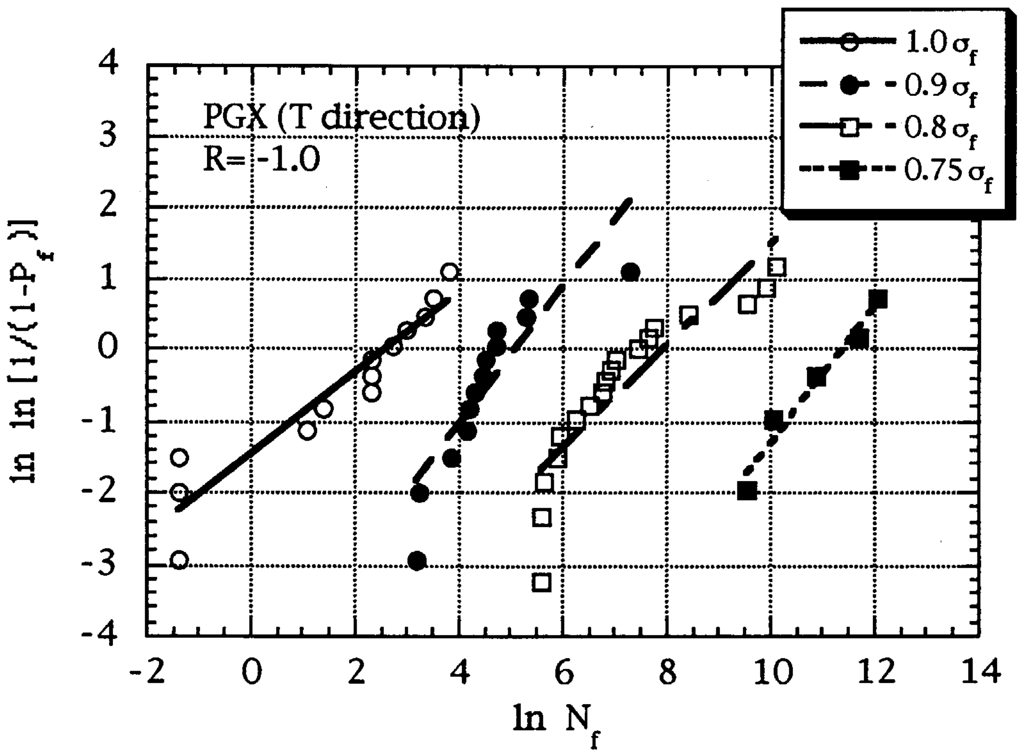

Fig.16(b) Plot of fatigue test data with R=-1.0 on PGX graphite (T-direction) for P-S-N analysis.

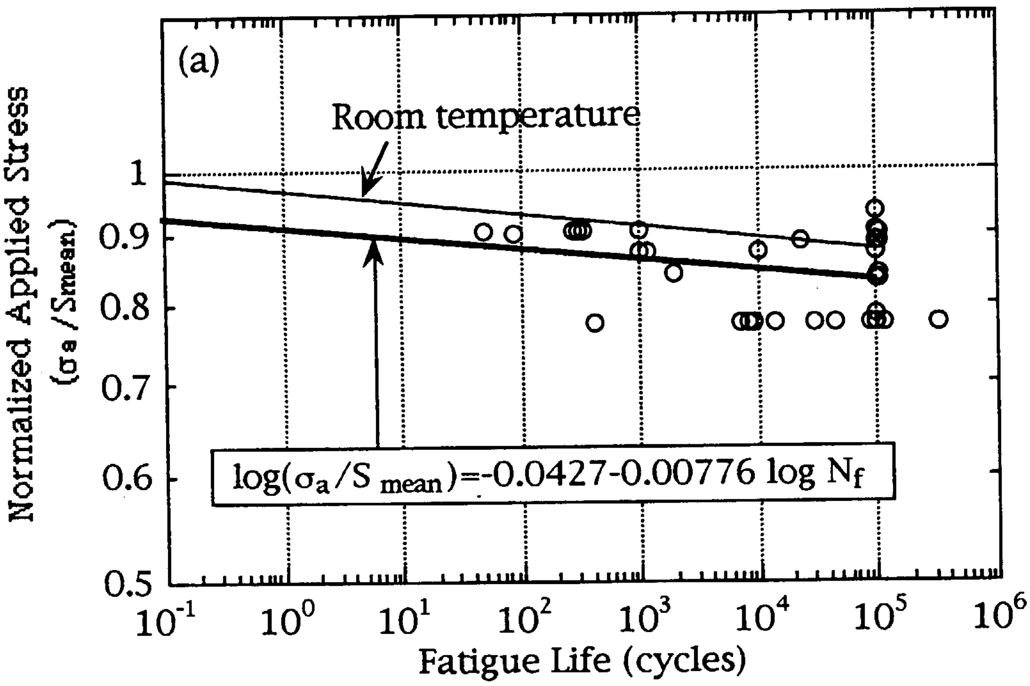

Fig.17(a) Constant fatigue life diagram for PGX graphite (L-direction), fatigue lines represent 99% survival probability with 95% confidence.

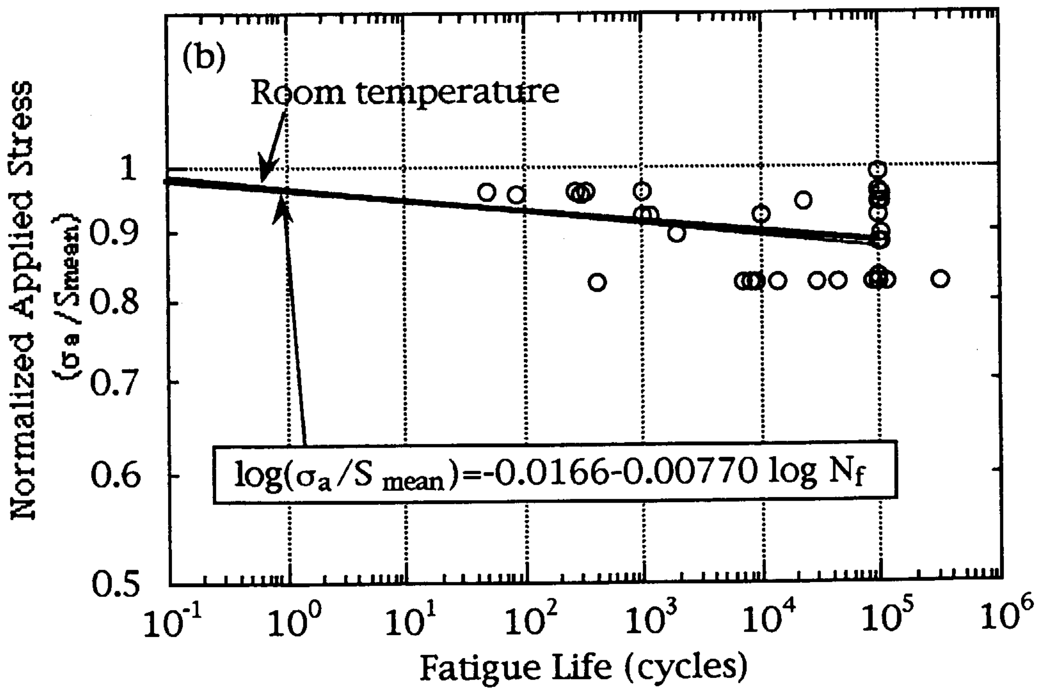

Fig.17(b) Constant fatigue life diagram for PGX graphite (T-direction), fatigue lines represent 99% survival probability with 95% confidence.

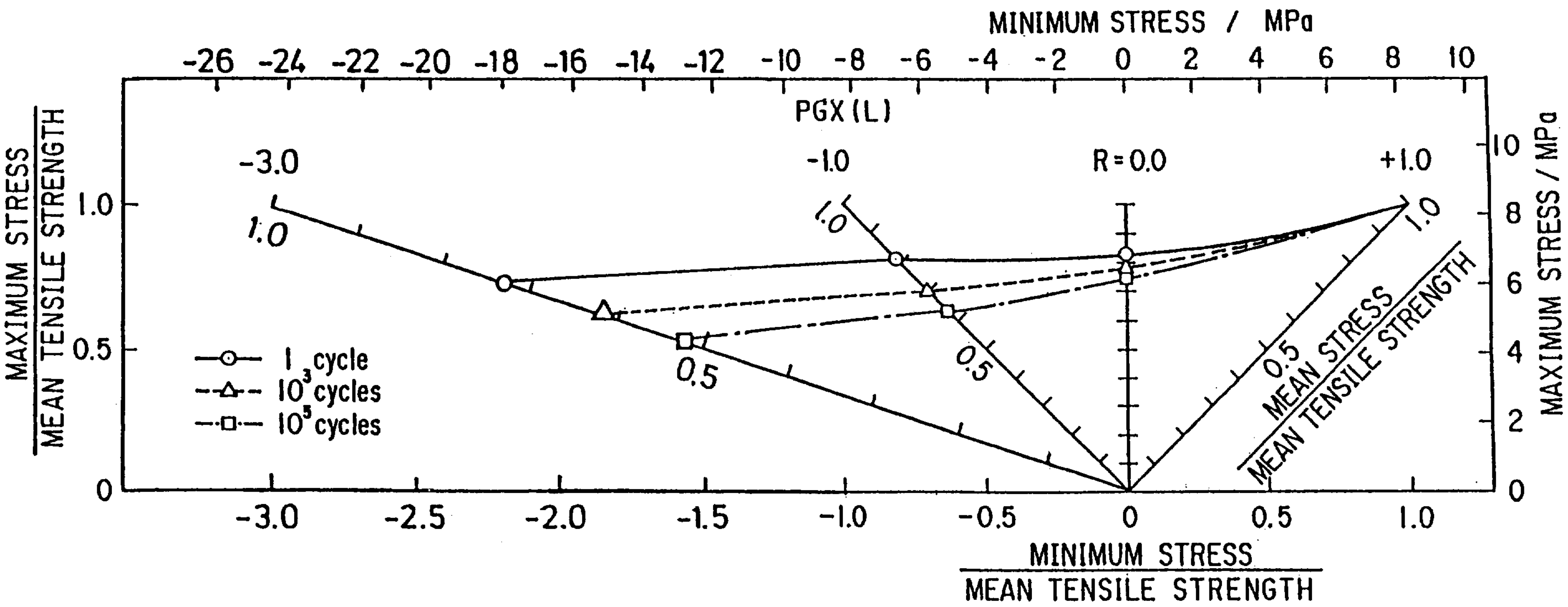

Fig.18(a) Constant fatigue life diagram for ASR-0RB carbon (L-direction), fatigue lines represent 99% survival probability with 95% confidence.

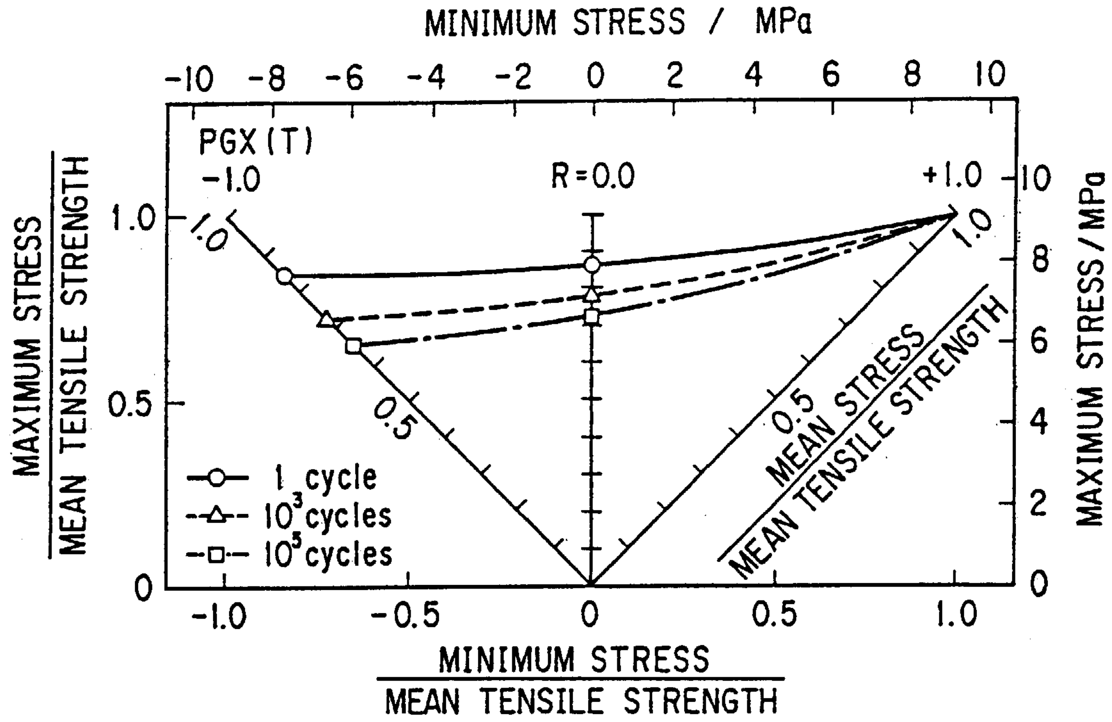

Fig.18(b) Constant fatigue life diagram for ASR-0RB carbon (T-direction), fatigue lines represent 99% survival probability with 95% confidence.

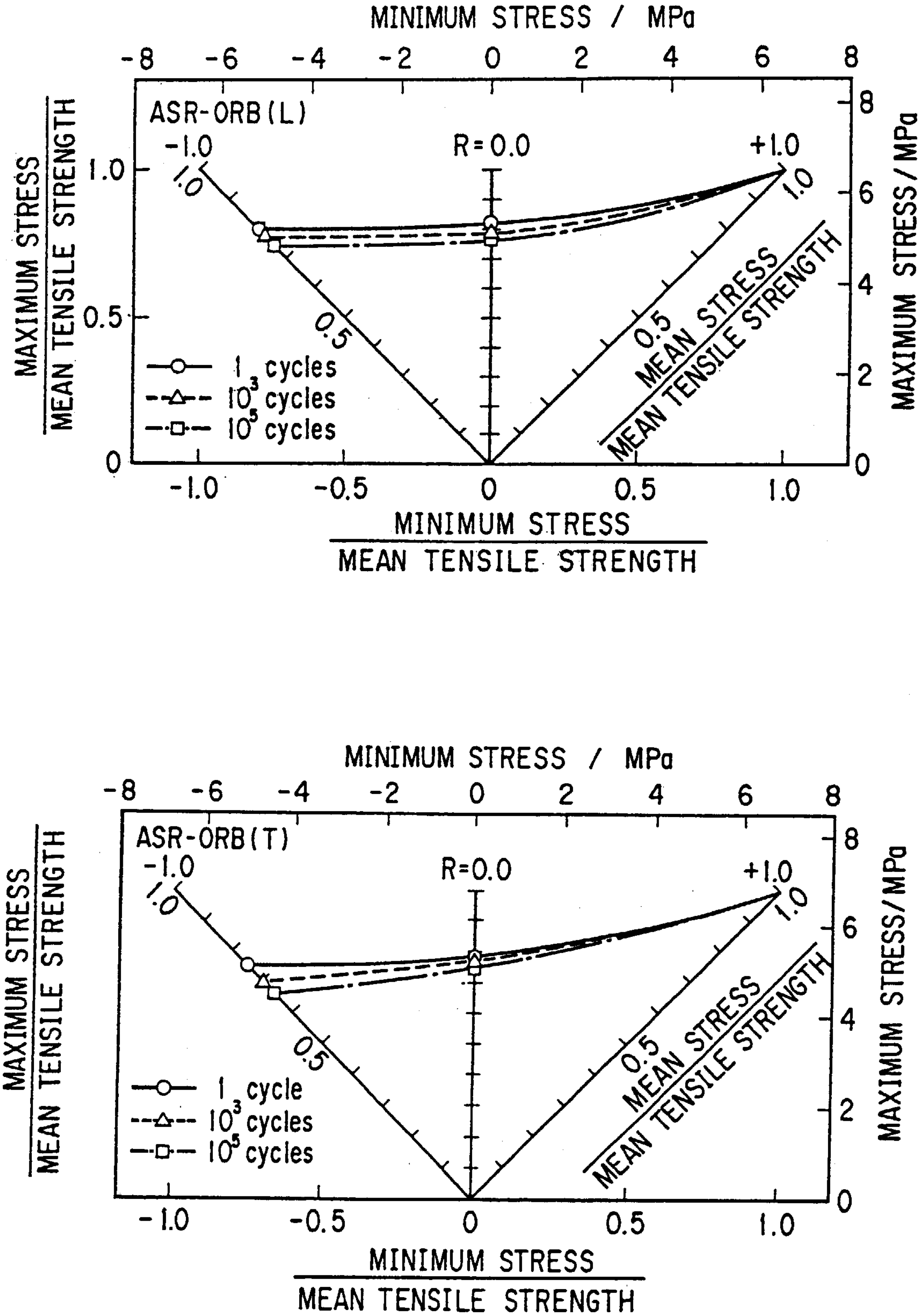

Fig.19 Fatigue strength of IG-11 graphite at 980℃ in vacuo, (a) applied stress normalized to the mean tensile strength at 980℃ and (b) applied stress normalized to the mean tensile strength at RT in vacuo.

Appendix: Digital Data on Static Strength and Fatigue Strength

Table A1 Tensile strength of PGX graphite (T)

No.	Tensile strength (MPa)		
	5mm D×10mm GL	10mm D×10mm GL	20mm D×10mm GL
1	8.86	8.15	9.34
2	9.50	9.17	7.68
3	9.11	8.94	8.41
4	8.49	8.14	8.18
5	9.14	8.80	7.51
6	8.90	10.03	9.03
7	8.99	9.80	8.99
8	9.44	8.64	8.23
9	9.30	9.47	8.51
10		9.10	8.70
Mean	9.08	9.02	8.46
Std. Dev.	0.32	0.63	0.59

Table A2 Tensile strength of PGX graphite (L)

No.	Tensile strength (MPa)		
	5mm D×10mm GL	10mm D×10mm GL	20mm D×10mm GL
1	8.18	8.84	8.49
2	9.96	7.26	8.91
3	8.51	8.17	8.83
4	5.29	7.61	7.09
5	7.43	6.43	6.69
6	6.94	5.78	4.64
7	7.72	6.64	6.29
8	7.63	8.31	8.60
9	8.05	6.90	8.47
10		8.65	
Mean	7.75	7.46	7.56
Std. Dev.	1.25	1.02	1.47

Table A3　　Compressive strength of PGX graphite (T)

No.	Compressive strength (MPa)				
	5mm D ×10mm L	10mm D ×20mm L	15mm D ×30mm L	30mm D ×60mm L	50mm D ×100mm L
1	29.08	31.38	31.84	31.87	30.91
2	30.98	31.76	32.05	31.91	31.99
3	30.55	31.15	30.95	30.57	28.11
4	30.97	31.11	31.31	32.11	30.85
5	28.04	29.42	30.42	28.26	30.46
6	27.69	30.09	30.85	32.96	32.93
7	28.40	30.88	31.55	32.24	31.95
8	28.74	31.53	31.86	30.77	27.88
9	25.27	26.63	27.44	30.60	30.69
10	25.66	26.90	27.19	31.19	30.32
11	31.21	32.88	32.77	29.81	
12	30.16	32.48	32.38	29.28	
13	29.88	30.85	31.84	29.91	
14	30.21	30.19	31.81	29.98	
15	28.72	30.07	30.62	30.15	
16	27.21	27.89	30.60	30.43	
17	28.95	29.68	30.44	32.20	
18	28.77	30.06	29.87	30.53	
19	31.08	30.07	30.33	31.65	
20	28.49	29.74	30.29	30.70	
Mean	29.00	30.24	30.82	30.86	30.61
Std. Dev.	1.69	1.63	1.43	1.16	1.60

Table A4 Compressive strength of PGX graphite (L)

No.	Compressive strength (MPa)				
	5mm D ×10mm L	10mm D ×20mm L	15mm D ×30mm L	30mm D ×60mm L	50mm D ×100mm L
1	30.07	31.28	31.02	31.44	30.91
2	28.81	29.99	31.12	31.21	32.63
3	29.77	30.32	31.06	31.37	30.18
4	30.31	31.38	32.09	31.01	29.80
5	28.81	29.83	31.45	31.07	30.93
6	29.47	29.55	31.04	30.69	30.55
7	28.94	29.80	31.01	31.07	30.23
8	30.65	30.27	30.75	31.90	31.86
9	30.45	30.68	30.68	31.83	31.93
10	28.39	30.47	30.77	31.63	32.03
11	27.18	30.79	31.57	32.84	
12	29.03	29.61	31.08	33.96	
13	30.54	32.64	32.94	32.55	
14	30.31	32.70	32.17	32.45	
15	29.43	29.38	30.83	29.53	
16	29.52	30.23	30.79	33.02	
17	29.47	30.81	30.68	28.91	
18	29.34	30.36	30.39	28.50	
19	29.53	30.79	31.83	30.97	
20	29.01	30.81	30.71	31.88	
Mean	29.45	30.59	31.20	31.39	31.11
Std. Dev.	0.84	0.90	0.63	1.33	0.95

Table A5 Results of tensile strength test on IG-11 graphite (L direction)

No.	Diameter (mm)	Young's modulus (GPa)	Tensile strength (MPa)
1	10.013	10.13	28.96
2	10.026	9.87	27.58
3	10.027	9.08	26.08
4	9.988	9.85	27.22
5	10.000	10.48	30.13
6	10.018	9.85	26.60
7	10.026	10.25	29.19
8	9.985	10.13	27.09
9	10.012	10.60	28.81
10	10.029	9.74	26.85
11	9.990	10.97	30.89
12	10.020	9.74	27.83
13	10.022	10.67	29.21
14	10.014	9.74	27.55
15	10.019	10.30	29.23
16	10.042	9.96	25.07
17	10.026	9.79	27.33
18	10.021	10.42	28.60
19	10.004	10.29	26.51
20	10.000	10.34	28.57
21	10.450	10.73	29.70
22	9.984	10.13	28.10
23	9.990	9.63	26.27
24	10.014	10.30	27.55
25	10.024	10.07	24.85
Average		10.12	27.83
Standard deviation		0.41	1.51

Table A6(a) Results of tensile strength test on PGX graphite (L direction)

No.	Diameter (mm)	Young's modulus (GPa)	Tensile strength (MPa)
1	10.023	6.65	8.89
2	10.220	6.64	9.07
3	10.004	6.61	8.25
4	10.023	6.71	8.42
5	10.011	6.58	8.57
6	10.027	6.44	8.01
7	10.013	6.61	8.13
8	10.019	6.49	8.18
9	10.017	6.61	8.90
10	10.029	6.77	7.23
11	10.025	6.58	7.95
12	9.998	6.65	8.68
13	10.015	6.68	8.78
14	9.965	6.83	8.08
15	10.023	6.80	9.12
16	10.040	6.61	8.52
17	9.984	6.76	8.55
18	10.025	6.49	7.88
19	10.016	6.61	7.24
20	10.020	6.58	9.05
21	10.021	6.80	6.62
22	10.009	6.80	7.77
23	10.025	6.64	7.08
24	10.019	6.73	7.83
25	10.006	6.83	7.09
26	10.014	6.52	7.03
27	10.022	6.67	7.43
28	10.001	6.67	7.88
29	9.972	6.67	8.33
30	9.997	6.42	7.95
31	9.987	6.55	9.50
32	10.016	6.32	7.50
33	10.019	6.52	8.60
34	10.060	6.59	8.83

No.	Diameter (mm)	Young's modulus (GPa)	Tensile strength (MPa)
35	10.068	6.46	8.92
36	10.025	6.64	9.09
37	10.017	6.40	8.46
38	10.044	6.52	9.26
39	10.013	6.21	8.23
40	10.019	6.77	9.19
41	10.000	6.64	8.58
42	10.022	6.67	9.17
43	10.038	6.52	8.43
44	10.043	6.71	8.39
Average		6.61	8.29
Standard deviation		0.14	0.70

Table A6(b) Results of tensile strength test on PGX graphite (T direction)

No.	Diameter (mm)	Young's modulus (GPa)	Tensile strength (MPa)
1	10.009	8.70	10.28
2	9.991	8.48	9.19
3	9.988	8.39	8.82
4	9.988	8.61	9.01
5	10.005	8.47	8.79
6	10.006	8.56	9.10
7	10.031	8.38	9.06
8	9.979	8.61	9.53
9	10.009	8.47	9.66
10	9.981	8.60	9.34
11	9.966	8.52	9.24
12	9.989	8.34	9.57
13	10.004	8.34	9.11
14	9.976	8.48	9.91
15	9.988	8.30	8.51
16	10.014	8.34	8.96
17	10.016	8.56	8.90
18	10.000	8.56	8.49
19	10.025	8.17	7.95
20	9.988	8.51	7.82
21	10.003	8.52	9.55
22	9.980	8.43	9.15
23	9.971	8.47	9.80
24	9.959	8.43	9.13
25	9.975	8.13	8.41
26	9.985	8.74	10.21
27	9.990	8.60	9.38
28	9.972	8.52	9.79
29	9.969	8.60	9.99
30	10.000	8.51	9.11
31	9.960	8.43	9.69
32	10.027	8.52	9.38
33	9.970	8.61	9.61
34	10.017	8.52	7.96
35	10.030	8.70	9.00
Average		8.49	9.18
Standard deviation		0.14	0.60

Table A7(a) Results of tensile strength test on ASR-0RB carbon (L direction)

No.	Diameter (mm)	Young's modulus (GPa)	Tensile strength (MPa)
1	9.990	9.73	5.00
2	9.980	9.73	7.08
3	10.000	9.46	6.77
4	10.000	9.06	5.53
5	10.000	10.01	7.12
6	9.980	9.78	6.58
7	9.980	9.72	7.21
8	10.000	9.45	7.02
9	9.980	9.56	6.83
10	9.970	8.95	6.34
11	9.990	9.15	6.76
12	10.010	9.63	6.67
13	10.010	9.20	5.92
14	10.000	9.78	6.99
15	10.010	9.72	7.17
16	10.010	9.72	5.89
17	9.970	8.95	6.41
18	9.990	9.29	6.57
19	10.000	9.05	6.02
20	10.000	9.09	6.37
Average		9.45	6.51
Standard deviation		0.33	0.59

Table A7(b) Results of tensile strength test on ASR-0RB carbon (T direction)

No.	Diameter (mm)	Young's modulus (GPa)	Tensile strength (MPa)
1	9.980	10.63	7.15
2	10.000	10.75	6.12
3	10.020	10.26	5.66
4	10.000	10.76	7.59
5	9.980	10.82	5.74
6	10.000	10.94	7.52
7	10.000	10.88	7.84
8	9.974	10.74	7.69
9	10.000	10.68	5.21
10	9.980	10.18	6.42
11	9.990	10.88	7.41
12	10.010	11.01	6.29
13	9.980	10.67	6.68
14	10.000	10.87	6.43
15	10.010	10.87	7.79
16	10.010	10.37	6.57
17	9.990	10.81	6.35
18	10.000	10.74	7.09
19	10.010	10.81	7.60
20	9.980	10.61	7.21
21	9.980	10.88	5.86
22	9.970	10.74	7.00
Average		10.72	6.78
Standard deviation		0.21	0.77

Table A8 Fatigue life data on IG-11 graphite (L direction)

R (Stress ratio) =-1.0
Mean tensile strength : 27.83 MPa

No.	Applied stress (MPa)	Number of cycles	No.	Applied stress (MPa)	Number of cycles
1	27.83	2	1	22.26	1045
2	27.83	2	2	22.26	1098
3	27.83	2	3	22.26	1154
4	27.83	2	4	22.26	1536
5	27.83	2	5	22.26	1677
6	27.83	3	6	22.26	1977
7	27.83	7	7	22.26	4111
8	27.83	10	8	22.26	7392
9	27.83	10	9	22.26	15710
10	27.83	22	10	22.26	31060
			11	22.26	56900
1	25.05	20	12	22.26	>103100
2	25.05	40			
3	25.05	45	1	20.87	9844
4	25.05	55	2	20.87	11590
5	25.05	63	3	20.87	15040
6	25.05	65	4	20.87	19350
7	25.05	80	5	20.87	25400
8	25.05	100	6	20.87	56690
9	25.05	106	7	20.87	27430
10	25.05	114	8	20.87	38440
11	25.05	157	9	20.87	99050
12	25.05	164	10	20.87	>105000
13	25.05	170	11	20.87	>110800
14	25.05	176	12	20.87	>112000
15	25.05	190	13	20.87	>121600
16	25.05	547			
17	25.05	816	1	19.48	>101800
			2	19.48	>105300
			3	19.48	>192600
			4	19.48	>217500
			5	19.48	>322200

Table A9(a) Fatigue life data on PGX graphite (L direction)

R (Stress ratio) =0.0
Mean tensile strength : 8.294 MPa

No.	Applied stress (MPa)	Number of cycles	No.	Applied stress (MPa)	Number of cycles
1	8.294	0.5	1	7.465	49
2	8.294	0.5	2	7.465	304
3	8.294	2	3	7.465	307
4	8.294	6	4	7.465	482
5	8.294	10	5	7.465	503
6	8.294	17	6	7.465	632
7	8.294	19	7	7.465	8328
8	8.294	20	8	7.465	1391
9	8.294	28	9	7.465	1846
10	8.294	37	10	7.465	8261
11	8.294	38	11	7.465	8501
12	8.294	45	12	7.465	9383
13	8.294	59			
14	8.294	70	1	7.050	437
15	8.294	90	2	7.050	10830
16	8.294	172	3	7.050	30290
17	8.294	359	4	7.050	99970
			5	7.050	>178100
1	7.879	0.5	6	7.050	>221600
2	7.879	2			
3	7.879	5	1	6.635	>126000
4	7.879	11	2	6.635	>130880
5	7.879	24	3	6.635	>191800
6	7.879	39	4	6.635	>207500
7	7.879	48			
8	7.879	94			
9	7.879	3336			
10	7.879	7396			

Table A9(b) Fatigue life data on PGX graphite (L direction)

R (Stress ratio) =-1.0
Mean tensile strength : 8.294 MPa

No.	Applied stress (MPa)	Number of cycles	No.	Applied stress (MPa)	Number of cycles
1	8.294	4	1	6.635	10
2	8.294	4	2	6.635	197
3	8.294	8	3	6.635	320
4	8.294	9	4	6.635	706
5	8.294	10	5	6.635	1146
6	8.294	11	6	6.635	1384
7	8.294	12	7	6.635	1982
8	8.294	12	8	6.635	2035
9	8.294	13	9	6.635	2151
10	8.294	14	10	6.635	2653
11	8.294	14	11	6.635	5898
12	8.294	17	12	6.635	10410
13	8.294	19	13	6.635	14940
14	8.294	21	14	6.635	39720
15	8.294	60	15	7.465	> 143500
1	7.465	9	1	5.806	6129
2	7.465	10	2	5.806	18080
3	7.465	11	3	5.806	> 144100
4	7.465	45	4	5.806	> 146100
5	7.465	52	5	5.806	> 147200
6	7.465	73			
7	7.465	95	1	4.976	> 140600
8	7.465	96			
9	7.465	105			
10	7.465	136			
11	7.465	147			
12	7.465	197			
13	7.465	271			
14	7.465	350			
15	7.465	622			
16	7.465	968			
17	7.465	2062			

Table A9(c) Fatigue life data on PGX graphite (L direction)

R (Stress ratio) =-3.0
Mean tensile strength : 8.294 MPa

No.	Applied stress (MPa)	Number of cycles	No.	Applied stress (MPa)	Number of cycles
1	8.294	2	1	5.806	715
2	8.294	2	2	5.806	835
3	8.294	3	3	5.806	1029
4	8.294	3	4	5.806	2050
5	8.294	6	5	5.806	2177
			6	5.806	5839
1	7.465	5	7	5.806	6698
2	7.465	8	8	5.806	24180
3	7.465	15			
4	7.465	18	1	5.391	14100
5	7.465	24	2	5.391	79330
6	7.465	27	3	5.391	> 102500
7	7.465	36	4	5.391	> 108200
			5	5.391	> 133700
1	6.635	64	6	5.391	> 135900
2	6.635	87	7	5.391	> 161500
3	6.635	88			
4	6.635	110			
5	6.635	148			
6	6.635	154			
7	6.635	161			

Table A10(a) Fatigue life data on PGX graphite (T direction)

R (Stress ratio) =0.0
Mean tensile strength : 9.183 MPa

No.	Applied stress (MPa)	Number of cycles
1	9.183	0.5
2	9.183	0.5
3	9.183	0.5
4	9.183	0.5
5	9.183	0.5
6	9.183	0.5
7	9.183	0.5
8	9.183	3
9	9.183	4
10	9.183	5
11	9.183	6
12	9.183	14
13	9.183	15
14	9.183	39
15	9.183	53
1	8.724	2
2	8.724	2
3	8.724	4
4	8.724	19
5	8.724	35
6	8.724	38
7	8.724	165
8	8.724	369
1	8.265	8
2	8.265	11
3	8.265	40
4	8.265	56
5	8.265	75
6	8.265	137
7	8.265	159
8	8.265	225

No.	Applied stress (MPa)	Number of cycles
9	8.265	233
10	8.265	311
11	8.265	332
12	8.265	360
13	8.265	414
14	8.265	621
15	8.265	627
16	8.265	664
17	8.265	715
18	8.265	1993
1	7.806	42
2	7.806	46
3	7.806	378
4	7.806	379
5	7.806	515
6	7.806	1268
7	7.806	1668
8	7.806	4854
9	7.806	8525
10	7.806	14230
11	7.806	25470
12	7.806	> 123500
13	7.806	> 168900
1	7.346	> 122800
2	7.346	> 153300
3	7.346	> 253500

Table A10(b) Fatigue life data on PGX graphite (T direction)

R (Stress ratio) =-1.0
Mean tensile strength : 9.183 MPa

No.	Applied stress (MPa)	Number of cycles	No.	Applied stress (MPa)	Number of cycles
1	9.183	0.25	1	7.346	262
2	9.183	0.25	2	7.346	267
3	9.183	0.25	3	7.346	278
4	9.183	3	4	7.346	365
5	9.183	4	5	7.346	377
6	9.183	10	6	7.346	512
7	9.183	10	7	7.346	680
8	9.183	10	8	7.346	894
9	9.183	15	9	7.346	940
10	9.183	20	10	7.346	1025
11	9.183	28	11	7.346	1128
12	9.183	32	12	7.346	1723
13	9.183	45	13	7.346	2040
			14	7.346	2342
1	8.265	24	15	7.346	4497
2	8.265	26	16	7.346	13660
3	8.265	48	17	7.346	19540
4	8.265	63	18	7.346	24970
5	8.265	67			
6	8.265	74	1	6.887	13860
7	8.265	87	2	6.887	23120
8	8.265	92	3	6.887	52800
9	8.265	110	4	6.887	>121600
10	8.265	114	5	6.887	>169400
11	8.265	200			
12	8.265	207	1	6.428	>118300
13	8.265	1467	2	6.428	>169100
			3	6.428	>289600

Table A11(a) Fatigue life data on ASR-0RB carbon (L direction)

R (Stress ratio) =0.0
Mean tensile strength : 6.512 MPa

No.	Applied stress (MPa)	Number of cycles
1	6.512	0.5
2	6.512	0.5
3	6.512	0.5
4	6.512	2
5	6.512	3
6	6.512	3
7	6.512	4
8	6.512	10
9	6.512	14
10	6.512	61
11	6.512	138
12	6.512	700
13	6.512	736
1	6.186	7
2	6.186	10
3	6.186	34
4	6.186	382
5	6.186	557
6	6.186	54110
1	5.861	60
2	5.861	675
3	5.861	3885
4	5.861	4254
5	5.861	6117
6	5.861	23930
7	5.861	50990
8	5.861	>333900
9	5.861	>385900

Table A11(b) Fatigue life data on ASR-0RB carbon (L direction)

R (Stress ratio) =-1.0
Mean tensile strength : 6.512 MPa

No.	Applied stress (MPa)	Number of cycles	No.	Applied stress (MPa)	Number of cycles
1	6.512	0.25	1	5.861	0.25
2	6.512	0.25	2	5.861	94
3	6.512	4	3	5.861	283
4	6.512	10	4	5.861	400
5	6.512	16	5	5.861	429
6	6.512	20	6	5.861	1300
7	6.512	28	7	5.861	14880
8	6.512	40	8	5.861	21490
9	6.512	124	9	5.861	43190
10	6.512	145	10	5.861	>124800
1	6.186	0.25	1	5.210	>111800
2	6.186	0.25	2	5.210	>114100
3	6.186	0.25	3	5.210	>115700
4	6.186	0.25	4	5.210	>196300
5	6.186	4			
6	6.186	52	1	4.558	>117300
7	6.186	56			
8	6.186	152			
9	6.186	195			
10	6.186	423			
11	6.186	615			

Table A12(a) Fatigue life data on ASR-0RB carbon (T direction)

R (Stress ratio) =0.0
Mean tensile strength : 6.783 MPa

No.	Applied stress(MPa)	Number of cycles
1	6.783	0.5
2	6.783	0.5
3	6.783	0.5
4	6.783	9
5	6.783	20
6	6.783	21
7	6.783	35
8	6.783	39
9	6.783	256
1	6.444	0.5
2	6.444	10
3	6.444	18
4	6.444	75
5	6.444	165
6	6.444	4781
7	6.444	16900
8	6.444	31530
9	6.444	35280
10	6.444	> 354800
1	6.105	553
2	6.105	19430
3	6.105	43130
4	6.105	> 108200
5	6.105	> 119400
6	6.105	> 127400
7	6.105	> 146100
8	6.105	> 150000

Table A12(b) Fatigue life data on ASR-0RB carbon (T direction)

R (Stress ratio) =-1.0
Mean tensile strength : 6.783 MPa

No.	Applied stress(MPa)	Number of cycles
1	6.783	0.25
2	6.783	0.25
3	6.783	0.25
4	6.783	0.25
5	6.783	3
6	6.783	3
7	6.783	20
8	6.783	423
1	6.105	125
2	6.105	238
3	6.105	1065
4	6.105	1474
5	6.105	2660
6	6.105	3190
7	6.105	6651
8	6.105	> 126700
1	5.776	72
2	5.776	357
3	5.766	2530
4	5.766	6701
5	5.766	23180
6	5.766	> 100500
7	5.766	> 115200
8	5.766	> 116200
1	5.426	2854
2	5.426	> 100000
3	5.426	> 117100
4	5.426	> 119900
5	5.426	> 125000
6	5.426	> 157100

Table A13 Results of the tensile and fatigue tests of IG-11 graphite

Specimen No.	Tensile strength (MPa)	Applied stress (MPa)	Normalized stress (σa/Smean)	Fatigue life (cycles)	Test condition
1(A)	43.5				980℃ in vacuo
2(A)	43.1				ditto
3(A)	42.7				ditto
4(A)		33.2	0.775	7000	980℃ fatigue in vacuo
5(A)		33.2	0.775	29880	ditto
6(A)		33.2	0.775	8090	ditto
7(B)		33.2	0.775	9240	ditto
8(B)		33.2	0.775	14070	ditto
9(B)		33.2	0.775	44650	ditto
10(B)		33.2	0.775	400	ditto
11(B)	42.3*	33.2	0.775	>114980	980℃ fatigue, RT in vacuo
12(B)	43.1				200℃ in vacuo×2h, RT in vacuo
13(C)		33.2	0.775	87900	980℃ fatigue in vacuo
14(C)		33.2	0.775	>321100	ditto
15(C)	41.9				200℃ in vacuo×2h, RT in vacuo
16(C)	29.9*	33.2	0.775	>100000	980℃ fatigue in vacuo, RT in air
17(C)	43.7				200℃ in vacuo×2h, RT in vacuo
18(C)	32.0				RT in air
19(4)	47.1				980℃ in vacuo
20(5)	39.9				ditto
21(1)	35.4				RT in air
22(2)	45.5				RT in vacuo
23(5')	38.3				ditto
24(4')	37.1				ditto
25(3)	42.3				200℃ in vacuo, RT in vacuo
26(8)	39.9*	35.6	0.832	>100000	980℃ fatigue, RT in vacuo
27(7)	39.7*	33.6	0.785	>100000	ditto
28(6)	39.9*	33.6	0.785	>100000	ditto
29(13)	40.7*	37.2	0.869	>100000	ditto

Specimen No.	Tensile strength (MPa)	Applied stress (MPa)	Normalized stress (σa/Smean)	Fatigue life (cycles)	Test condition
30(10)	40.7*	39.9	0.932	>100000	980℃ fatigue, RT in vacuo
31(C9)	40.3*	36.0	0.841	>103570	ditto
32(D2)	40.5*	36.0	0.841	>104920	ditto
33(C2)	40.3*	35.6	0.832	>101010	ditto
34(D3)	40.8*	36.0	0.841	>104560	ditto
35(D5)	41.9*	37.2	0.869	>100090	ditto
36(D6)	40.4*	37.2	0.869	>100440	ditto
37(C5)	43.1*	38.7	0.904	>100050	ditto
38(C7)	42.3*	38.0	0.888	>104430	ditto
39(D12)	42.0*	38.0	0.888	>100320	ditto
40(D14)	42.9*	38.5	0.899	>102840	ditto
41(D7)		38.0	0.888	23160	980℃ fatigue
42(D8)		38.7	0.904	980	ditto
43(D9)		38.7	0.904	330	ditto
44(D10)		38.7	0.904	50	ditto
45(C10)		38.7	0.904	270	ditto
46(D13)		38.5	0.899	88	ditto
47(D15)		38.6	0.902	300	
48(C1)	41.1				980℃ in vacuo
49(D1)	41.5				ditto
50(C8)	43.1				ditto
51(D6)	37.2*	37.2	0.869	>100440	ditto
52(12)		37.2	0.869	1170	980℃ fatigue
53(11)		37.2	0.869	10200	ditto
54(C4)		36.0	0.841	1950	ditto
55(D4)		37.2	0.869	1000	ditto

*) Specimens tensile-tested after fatigue cycles more than 10^5.

国際単位系 (SI) と換算表

表1　SI基本単位および補助単位

量	名　称	記　号
長　さ	メートル	m
質　量	キログラム	kg
時　間	秒	s
電　流	アンペア	A
熱力学温度	ケルビン	K
物質量	モル	mol
光　度	カンデラ	cd
平面角	ラジアン	rad
立体角	ステラジアン	sr

表2　SIと併用される単位

名　称	記　号
分，時，日	min, h, d
度，分，秒	°, ′, ″
リットル	l, L
トン	t
電子ボルト	eV
原子質量単位	u

$1\ eV = 1.60218 \times 10^{-19} J$

$1\ u = 1.66054 \times 10^{-27} kg$

表5　SI接頭語

倍数	接頭語	記　号
10^{18}	エクサ	E
10^{15}	ペタ	P
10^{12}	テラ	T
10^{9}	ギガ	G
10^{6}	メガ	M
10^{3}	キロ	k
10^{2}	ヘクト	h
10^{1}	デカ	da
10^{-1}	デシ	d
10^{-2}	センチ	c
10^{-3}	ミリ	m
10^{-6}	マイクロ	μ
10^{-9}	ナノ	n
10^{-12}	ピコ	p
10^{-15}	フェムト	f
10^{-18}	アト	a

表3　固有の名称をもつSI組立単位

量	名　称	記号	他のSI単位による表現
周波数	ヘルツ	Hz	s^{-1}
力	ニュートン	N	$m\cdot kg/s^2$
圧力，応力	パスカル	Pa	N/m^2
エネルギー，仕事，熱量	ジュール	J	N·m
工率，放射束	ワット	W	J/s
電気量，電荷	クーロン	C	A·s
電位，電圧，起電力	ボルト	V	W/A
静電容量	ファラド	F	C/V
電気抵抗	オーム	Ω	V/A
コンダクタンス	ジーメンス	S	A/V
磁束	ウェーバ	Wb	V·s
磁束密度	テスラ	T	Wb/m^2
インダクタンス	ヘンリー	H	Wb/A
セルシウス温度	セルシウス度	℃	
光束	ルーメン	lm	cd·sr
照度	ルクス	lx	lm/m^2
放射能	ベクレル	Bq	s^{-1}
吸収線量	グレイ	Gy	J/kg
線量当量	シーベルト	Sv	J/kg

表4　SIと共に暫定的に維持される単位

名　称	記　号
オングストローム	Å
バーン	b
バール	bar
ガル	Gal
キュリー	Ci
レントゲン	R
ラド	rad
レム	rem

$1\ Å = 0.1\ nm = 10^{-10} m$

$1\ b = 100\ fm^2 = 10^{-28} m^2$

$1\ bar = 0.1\ MPa = 10^5 Pa$

$1\ Gal = 1\ cm/s^2 = 10^{-2} m/s^2$

$1\ Ci = 3.7 \times 10^{10} Bq$

$1\ R = 2.58 \times 10^{-4} C/kg$

$1\ rad = 1\ cGy = 10^{-2} Gy$

$1\ rem = 1\ cSv = 10^{-2} Sv$

(注)

1. 表1－5は「国際単位系」第5版，国際度量衡局 1985年刊行による。ただし，1 eVおよび1 uの値はCODATAの1986年推奨値によった。
2. 表4には海里，ノット，アール，ヘクタールも含まれているが日常の単位なのでここでは省略した。
3. barは，JISでは流体の圧力を表わす場合に限り表2のカテゴリーに分類されている。
4. EC閣僚理事会指令ではbar，barnおよび「血圧の単位」mmHgを表2のカテゴリーに入れている。

換　算　表

力	$N(=10^5 dyn)$	kgf	lbf
	1	0.101972	0.224809
	9.80665	1	2.20462
	4.44822	0.453592	1

粘　度　$1\ Pa\cdot s(N\cdot s/m^2) = 10\ P$(ポアズ)$(g/(cm\cdot s))$

動粘度　$1\ m^2/s = 10^4 St$(ストークス)(cm^2/s)

圧力	MPa(=10 bar)	kgf/cm^2	atm	mmHg(Torr)	lbf/in^2(psi)
	1	10.1972	9.86923	7.50062×10^3	145.038
	0.0980665	1	0.967841	735.559	14.2233
	0.101325	1.03323	1	760	14.6959
	1.33322×10^{-4}	1.35951×10^{-3}	1.31579×10^{-3}	1	1.93368×10^{-2}
	6.89476×10^{-3}	7.03070×10^{-2}	6.80460×10^{-2}	51.7149	1

エネルギー・仕事・熱量	$J(=10^7 erg)$	kgf·m	kW·h	cal(計量法)	Btu	ft·lbf	eV
	1	0.101972	2.77778×10^{-7}	0.238889	9.47813×10^{-4}	0.737562	6.24150×10^{18}
	9.80665	1	2.72407×10^{-6}	2.34270	9.29487×10^{-3}	7.23301	6.12082×10^{19}
	3.6×10^6	3.67098×10^5	1	8.59999×10^5	3412.13	2.65522×10^6	2.24694×10^{25}
	4.18605	0.426858	1.16279×10^{-6}	1	3.96759×10^{-3}	3.08747	2.61272×10^{19}
	1055.06	107.586	2.93072×10^{-4}	252.042	1	778.172	6.58515×10^{21}
	1.35582	0.138255	3.76616×10^{-7}	0.323890	1.28506×10^{-3}	1	8.46233×10^{18}
	1.60218×10^{-19}	1.63377×10^{-20}	4.45050×10^{-26}	3.82743×10^{-20}	1.51857×10^{-22}	1.18171×10^{-19}	1

1 cal = 4.18605 J (計量法)

　= 4.184 J (熱化学)

　= 4.1855 J (15 °C)

　= 4.1868 J (国際蒸気表)

仕事率　1 PS (仏馬力)

　= 75 kgf·m/s

　= 735.499 W

放射能	Bq	Ci
	1	2.70270×10^{-11}
	3.7×10^{10}	1

吸収線量	Gy	rad
	1	100
	0.01	1

照射線量	C/kg	R
	1	3876
	2.58×10^{-4}	1

線量当量	Sv	rem
	1	100
	0.01	1

(86年12月26日現在)

THE FATIGUE STRENGTH OF GRAPHITE AND CARBON MATERIALS FOR HTTR CORE COMPONENTS